LOW COST OPTICAL PRESSURE SENSOR USING FLEXIBLE PDMS GRATING

A DISSERTATION

Submitted in partial fulfilment of the requirements for the award of the degree

of

MASTER OF TECHNOLOGY

in

PHYSICS (PHOTONICS)

by

SAGAR KUMAR VERMA

(17560006)

DEPARTMENT OF PHYSICS
INDIAN INSTITUTE OF TECHNOLOGY ROORKEE
ROORKEE–247667 (INDIA)
JUN, 2019

INDIAN INSTITUTE OF TECHNOLOGY ROORKEE

****CONTENTS****

DECLERATION--- **c**
ACKNOWLEDGEMENT--- d
ABSTRACT--- e
LIST OF FIGURES--- f

Chapter 1 -Introduction

1. Sensor (1)
    1.1 Criteria to choose a Sensor (2)
    1.2 Pressure Sensor (3)
    1.3 Current Methods (4)
    1.4 Design of Low Cost Optical Pressure Sensor and its Working (6)
    1.5 Advantages of Optical Pressure Sensor (7)
    1.6 Application of Optical Pressure Sensor (8)
2. PDMS Flexible Grating (8)
    2.1 Polydemthylsiloxane (PDMS) (8)
    2.3 Mechanical properties of PDMS (8)
    2.3 Diffraction Grating (9)
    2.4 Working Principle of Diffraction Grating (10)
3. Photodiode (11)
    3.1 Quantum efficiency of Photodiode (12)
    3.2 Hybrid Perovskite Photodiode (12)
    3.3 Hybrid Perovskite Material (13)
    3.4 Tolerance Factor (13)

Chapter 2 –Experimental & Characterization Techniques

1. Scanning Electron Microscope (SEM) (15)
    1.1 Principle of SEM (16)
    1.2 Applications of SEM (16)
2. Atomic Force Microscope (AFM) (16)
    2.1 Working of AFM (16)
    2.2 Application of AFM (17)
3. Spin coating (18)

Chapter 3 -Transducer

1. Flexible PDMS Grating (20)
    1.1 Methodology for PDMS Grating (20)
2. Characterization of PDMS Grating (21)
3. Optical Characterization of PDMS Grating (27)
4. Grating Height variation with dip time in IPA (28)
5. Calculation for Longitudinal Pressure (29)
    5.1 Calculation for Strain in PDMS Grating (30)
    5.2 Observation of Strain in PDMS Grating (31)
    5.3 Calculation for Pressure on PDMS Grating (36)
        5.3.1 For 1.4 µm grating pitch (36)
        5.3.2 For 0.7 µm grating pitch (38)

Chapter 4–Detector

1. Schematic of Perovskite Photodiode (41)
2. Energy band diagram of Perovskite Photodiode (41)
3. Methodology (42)
4. Surface Morphology Characterization (45)
    4.1 FE-SEM Characterization (46)
    4.2 AFM Characterization (47)
5. UV-Visible Absorption (49)
6. Electrical Characterization (52)
    6.1 I-V under Forward bias (52)
    6.2 Photocurrent Generation (53)
7. Degradation of $MAPbBr_3$ under direct light Illumination (55)

Chapter 5–Conclusion and Future Scope

1. Conclusion (57)
2. Future Scope (58)

Bibliography

(60-63)

DEDICATED TO MY

BROTHR

ACKNOWLEDGEMENT

I would like to express enormous amount of gratitude, thanks and respect to my project supervisor **Dr. Monojit Bag**, Associate Professor, Department of Physics, **IIT ROORKEE**, for his aspiring guidance, encouraging support and invaluably constructive criticism throughout my project. He not only introduced me to the world of research but also helped me in my technical knowledge. His ideas always helped me to work in the right direction, without his support I would have never made it this far.

I am very thankful to **Dr. Kanhaiya Lal Yadav**, the Head of the Department for providing a very nice environment in our Department.

I would like to say special thanks to **Dr. Sachin Kumar Srivastava** for his enormous amount of help and support in my project work.

I am ever grateful to **Mr. Naveen Kumar Tailor, Mr. Ramesh Kumar, Mr. Jitendra Kumar** (Research Scholar) for assisting me and helping me in every possible way. During my working days, they provide a great learning and good atmosphere in our research group.

I would also like to thank my family members for their love and care throughout this endeavour.

SAGAR KUMAR VERMA

(17560006)

ABSTRACT

Pressure is a fundamental physical quantity or parameter which is used in field of sensor applications. Pressure sensors are used for different perspective in various field of research and industry. It has great interest in different of application like health care, automotive industries, aerospace industries and down-hall monitoring in oil wells. At present, there are many types of pressure sensors available like piezo-resistive sensor, capacitive type pressure, piezoelectric sensor but optical pressure sensors have different properties as high sensitivity, light weight, small size, environmental ruggedness, low cost compared with existing pressure sensors. We have designed the low cost optical pressure sensor using Polydimthylsiloxane (PDMS) an elastomeric polymer having 10:1 base and its cross linker regent network, based flexible grating which are crack free and durable and hybrid perovskite material Methyl-lade tri bromide ($MAPbBr_3$) based Photodetector because perovskite or hybrid perovskite materials are highly light emitter and absorber due to its energy band gap tuneable flexibility and these are highly light sensitive materials. The range of applied pressure on the PDMS grating of 1.4µm grating pitch and 160nm grating depth is 0 to 0.3945MPa and sensitivity is 0.0263MPa^{-1}.Similarly the applied pressure range on PDMS grating having grating pitch 0.7µm and grating depth 50nm is 0 to 0.337692MPa and Sensitivity is 0.0263MPa^{-1}.Such type of sensor can be used in the treatment of neurological disorder problems like headache and blood pressure.

List of Figures

Fig-1.1 Schematic of a general sensor (1)

Fig-1.2 Schematic of Piezoresistive Pressure Sensor (4)

Fig-1.3 Schematic of Capacitive Pressure Sensor (5)

Fig-1.4 Schematic of Piezoelectric Pressure Sensor (5)

Fig-1.5 Schematic of Low Cost Optical Pressure Sensor Using Flexible Grating (6)

Fig- 1.6 (a) Chemical structure of PDMS and (b) 3D view of PDMS molecular chain (8)

Fig-1.7 Normal Grating Spectrum (9)

Fig-1.8 Working principle of an ideal Grating (10)

Fig-1.9 Schematic of normal Photodiode (11)

Fig-1.10 Schematic of Perovskite crystal (12)

Fig-2.1 Schematic of SEM working (15)

Fig-2.2 Schematic of AFM working (17)

Fig-2.3 Schematic of Spin coater working (18)

Fig-3.1 Silicone elastomer base and its curing regent (20)

Fig-3.2 Picture of flexible PDMS grating (21)

Fig-3.3 For 20 minute in IPA dip AFM result (21)

Fig-3.4 For 30 minute in IPA dip AFM result (22)

Fig-3.5 For 40 minute in IPA dip AFM result (23)

Fig-3.6 For 50 minute in IPA dip AFM result (24)

Fig-3.7 For 60 minute in IPA dip AFM result (25)

Fig-3.8 For DVD pattern AFM result (22)

Fig-3.9 Optical arrangement to record the response of PDMS grating for different light source with stretching of grating. (28)

Fig-3.10 Grating height V/s IPA dipping time (28)

Fig-3.11 Photon count or density variation with strain induced in grating having 1.4 µm grating pitch (31)

Fig-3.12 (a) and (b) is for particular wavelength for highest peak in spectrum as 541 nm and plot it with the strain in photon density mode. (31)

Fig-3.13 (a) and (b) is for particular wavelength as 541 nm and plot it with the strain in transmission mode. (32)

Fig-3.14 Photon intensity or density variation with strain induced in grating having 0.7µm grating pitch (33)

Fig-3.15 (a) and (b) For particular wavelength for highest peak in spectrum as 541 nm and plot it with the strain in photon density mode (33)

Fig-3.16 (a) and (b) For particular wavelength as 541 nm and plot it with the strain in transmission mode (34)

Fig-3.17 (a), (b) For particular wavelength as 541 nm and plot it with the strain in transmission mode for simple PDMS film (35)

Fig-3.18 Variation in pressure with the increase in induced strain in PDMS grating of pitch 1.4 µm. (36)

Fig-3.19 Change in pressure with change in induced strain in PDMS grating for 0% to 15% change in strain for grating pitch 1.4 µm. (37)

Fig-3.20 Variation in pressure with the change in induced strain in PDMS film for grating pitch 0.7 µm (38)

Fig-3.21 Variation in pressure with change in induced strain in PDMS grating for 0% to 13% change in strain for grating pitch 0.7µm. (39)

Fig-4.1 Schematic geometry of different combination and their energy band diagram with electron hole migration under reverse bias condition (42)

Fig-4.2 (1) Optical image of successive film deposited on substrates ITO and FTO (2) Optical image of perovskite photodiode for different geometry as mentioned above (a), (b), (c), (d), (45)

Fig-4.3 (a.1) and (a.2) FE-SEM images of surface morphology for $ITO/MAPbBr_3$ (46)

Fig-4.4 (b.1) and (b.2) FE-SEM images of surface morphology for $ITO/PEDOT:PSS/MAPbBr_3$ (46)

Fig-4.5 (c.1) and (c.2) FE-SEM images of surface morphology for $FTO/TiO_2/MAPbBr_3$ (47)

Fig-4.6 (a.1) and (a.2) AFM images of surface morphology for $ITO/MAPbBr_3$ (47)

Fig-4.7 (b.1) and (b.2) AFM images of surface morphology for $ITO/PEDOT:PSS/MAPbBr_3$ (48)

Fig-4.8 (c.1) and (c.2) AFM images of surface morphology of $FTO/TiO_2/MAPbBr_3$ (48)

Fig-4.9 Absorbance spectrum of $MAPbBr_3$ film on different substrate as mentioned in graph. (49)

Fig-4.10 (a) Absorption spectrum of $MAPbBr_3$ film on ITO substrate and

(b) Corresponding Tauc plot (50)

Fig-4.11 (a) Absorption spectrum of $MAPbBr_3$ film on PEDOT:PSS coated substrate and (b) Corresponding Tauc Plot (51)

Fig-4.12 (a) Absorption spectrum of $MAPbBr_3$ film on TiO_2 coated FTO substrate and (b) Corresponding Tauc plot (52)

Fig-4.13 (a) and (b) I-V characteristics of perovskite diode in range -5V to 5V. (53)

Fig-4.14 (a) and (b) Photocurrent generation in perovskite devices under the light illumination in reverse bias condition for 0V to -5V biasing range (54)

Fig-4.15 Direct effect of light on hybrid perovskite film (55)

CHAPTER-1

INTRODUCTION

1 SENSOR

The sensor is a device in which change in any physical parameter as temperature, pressure, and others at the input end provides the corresponding change at the output and of the device in the form of another physical parameter, e.g. electrical, an optical signal, etc [1]. In modern life we are dealing with sensor technology, we are living in a sensor world as example our mobile phone is the best example of our dependence on sensor technology because there are so many types of sensor are embedded in new generation mobile technology like blood pressure sensor, temperature sensor, humidity sensor, light sensor or fingerprint and eye sensor and many more sensors are embedded in it [2]. There is four major part of a sensor which are an analyte, receptor, transducer and detector [4].

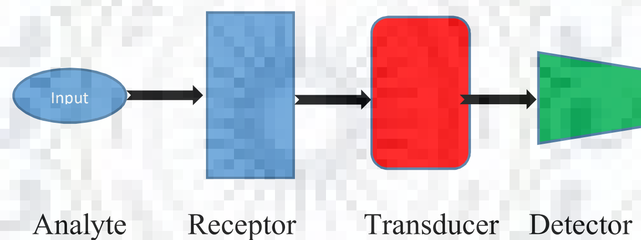

Fig-1.1- Schematic of a general sensor

Mostly available commercial sensors convert physical phenomena into an electrical signal or optical signal. Some important elements of the sensor are as below-

Input Element

The element of a sensor that feeds the input signal in the form of change in some physical parameter to the transducer is called an input device or element of a sensor. There are two types of the input element in case of sensor technology

(a) Interfering Input

The input that response to the sensor as the linear superposition of measured variables.

(b) Modifying Input

Those that change the behavior of a sensor with respect to the calibration curve.

Transducer

It is an active element of a sensor that converts one form of energy to another. When an input is a physical quantity and output is electrical or optical, it works as a Sensor and when input is electrical or optical and output a physical quantity, it works as Actuator [3-4].

Output Device

The element of a sensor which produces the result in the form of electrical or optical data for the change in physical parameter made at the input end of the device.

So many types of sensors are available now in the market and we can classify sensor technology in various ways, some general types of sensor

(a) Temperature sensor
(b) Pressure sensor
(c) Light sensor
(d) Humidity sensor
(e) Strain sensor
(f) Proximity sensor

And many more types of sensors are available in markets depending upon the demand of human beings to make their life smooth and easier

1.1 Criteria to choose a Sensor

These are the important features that have to be considered when a person goes to choose a sensor according to his needs. Specific characteristics can be classified by three major factors as

(a) Environmental Factor

A sensor should be environment-friendly and it should have cared for these factors

1. Temperature range
2. Humidity effects of sensor
3. Corrosion effects of sensor
4. Size of the sensor
5. Ruggedness of sensor
6. Power consumption by sensor
7. Self-test capability of the sensor

(b) Sensor Characteristics

A sensor should have the following characteristics to predict its specifications

1. **Accuracy**- It is the capacity of the instrument to measure the result accurately as much as close to its true or actual value.
2. **Discrimination-** It is the minimal change of the input necessary to produce a detectable change at the output. It is also known as Resolution and when the increment is from zero, it is called Threshold.
3. **Precision-** The capacity of a measuring instrument to give the same reading when repetitively measuring the same quantity under the same prescribed conditions. Precision is a necessary but not sufficient condition for accuracy.
4. **Repeatability-** The reading that varies is repeatedly measured under the same environment.
5. **Calibration-** Essential for most of the measuring devices as the readings changes with time.
6. **Range-** It should be the defined measurement limit or range of the sensor.
7. **Response time-** Response time to detect the change at the input end and to produce the output should be small as much as possible.
8. **Calibration-** Essential for most of the measuring devices as the readings changes with time

(c) Economical Factor

Economical factors play an important role in using a sensor as given below-

(a) Cost

(b) Availability

(c) Lifetime

1.2 Pressure Sensor

Pressure sensors are used for a different perspective in various fields of research and industry. It has a great interest in different applications like health care, automotive industries, aerospace industries and down-hall monitoring in oil wells [5-6]. At present, there are many types of pressure sensors available like a piezo-resistive sensor, capacitive type pressure, piezoelectric sensor but optical pressure sensors have different properties which makes it superior to other technologies [7]. But the flexible pressure sensors have

various important properties to make it different from other trending sensor technology and have versatile applications in the next generation of flexible electronics.

1.3 Current Methods

The following electromechanical based pressure sensor technologies are majorly being used for pressure sensing currently:-

(a) Piezoresistive Type

In metal diaphragm-based pressure sensors, the method which is commonly used is to locate metal strain gauges (foil type) on the metal diaphragm, in positions of maximum stress to maximize the sensitivity [7]. Due to piezoresistive property in Silicon, and silicon micromachining for diaphragm realization, boron-doped silicon piezoresistors have replaced the metal strain gauges [8]. The much higher sensitivities have been achieved due to the direct embedding of piezoresistors on the silicon diaphragm by implanting or diffusing boron in the selected portion of maximum stress as shown in Fig.

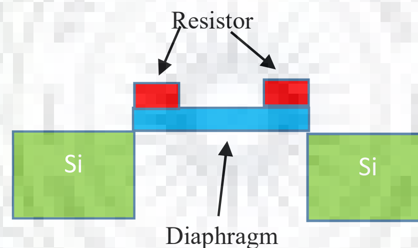

Fig-1.2 Schematic of Piezoresistive pressure sensor

These resistors are connected in the form of a Whetstone Bridge that provides an output when the resistors are strained under the action of the pressure sensed by the diaphragm. Subsequent sections deal with the enabling of linear operation over a low range of pressure by piezoresistive type [9]. As a result, they have captured the major market of pressure sensors encompassing the automobile industry, defense, space as well as biomedical applications.

(b) **Capacitive Type**

A schematic diagram of a silicon micromachined sensor of this type is shown in the figure. This approach uses the diaphragm as one electrode of a parallel plate capacitor structure and diaphragm displacement causes a change in capacitance with respect to a fixed electrode [10-11]. The merits of capacitive pressure sensors are their high sensitivity, which is practically invariant with temperature. [12]. An additional disadvantage of this approach is the nonlinear relationship between the capacitance and displacement and hence a force-balancing and linearizing electronic circuit is essential to capture a wide range of pressures.

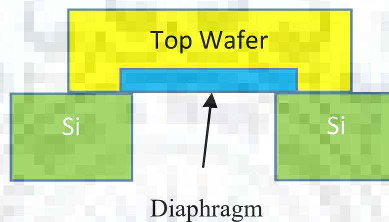

Fig-1.3 Schematic of Capacitive pressure sensor

(c) **Piezoelectric Type:-**

Silicon does not have a piezoelectric effect [13]. So piezoelectric sensing elements, such as Lead Zirconate Titanate (PZT) or Zinc Oxide (ZnO) are placed/deposited on to the silicon diaphragm as shown in Figure

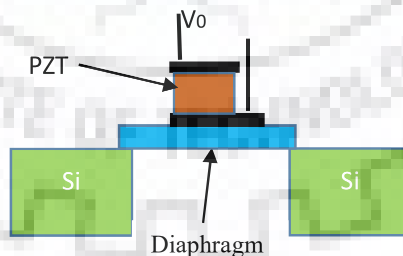

Fig-1.4 Schematic of Piezoelectric pressure sensor

The deflection of the diaphragm induces strain in the piezoelectric material and hence a charge is provided [14-15]. These sensors are suitable only for measuring dynamic pressure and are not suitable for static pressure sensing because piezoelectric materials respond only

to changing strains [16]. The major advantage of this approach is that an external power supply is not required.

In this work, we have mainly focused on the low cost of the optical pressure sensor using polydimethylsiloxane (PDMS) polymer based flexible grating to use as deflecting diaphragm and hybrid perovskite material based Photodetector. We have chosen a hybrid perovskite material based photodetector to record the signal in the form of Photocurrent due to having high absorptive, an emissive and good light sensitive property of perovskite materials.

1.4 Design of Low- Cost Optical Pressure Sensor and it's Working

the following one is the purposed design of our low -cost optical pressure sensor. A green laser will be used because of its monochromatic and directional nature. This monochromatic light will pass through an aperture having its diameter approximately 0.2mm or smaller as much as possible to make the light spot size as point-like spot size. After passing through the aperture light will fall on the PDMS grating where it will get diffracted.

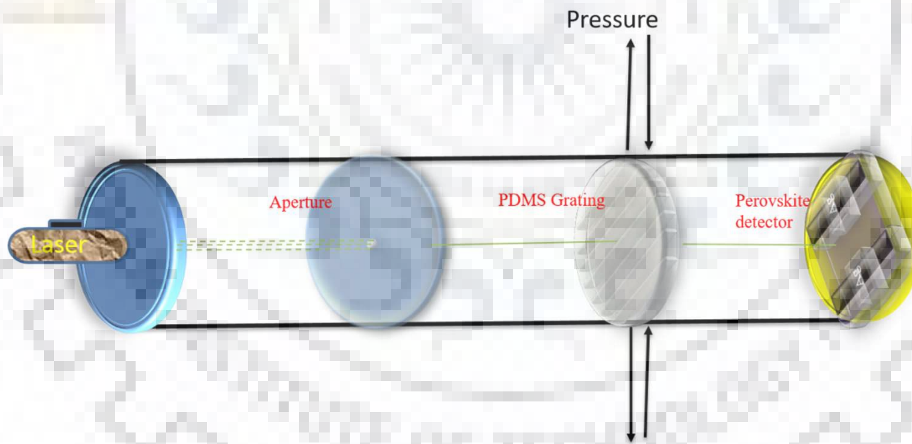

Fig 1.5- Schematic of low-cost optical pressure sensor using a flexible grating

When the pressure will be applied on the PDMS grating, the pitch of the grating will be changed due to one novel property named as the flexibility of PDMS film [17]. As the grating pitch will change the number of a light photon passing through the grating spacing will change which will be detected by hybrid perovskite material $MAPbBr_3$ or methylammonium lead tri-bromide based photodetector.T his light passing through the PDMS grating will be absorbed by the Perovskite photodiode and photocurrent will be

generated through the photodetector. The generated photocurrent will change with the corresponding change in applied pressure on the PDMS grating. Thus the change in applied pressure will be recorded in the form of Photocurrent as a detecting signal.

1.5 Advantages of Optical Pressure Sensor

At present, there are many types of pressure sensors available like a piezo-resistive sensor, capacitive type pressure, piezoelectric sensor but optical pressure sensors have different properties like

(a) Electromagnetic interference immunity
(b) High sensitivity
(c) Lightweight
(d) Small size
(e) Environmental ruggedness
(f) Low cost and multiplexing and distributed capacity compared with existing pressure sensors

1.6 Applications of Optical Pressure Sensor

Pressure and change in pressure is the most important and fundamental law or concept of physics which is strictly involved in science and research field as well as in our daily life. On the base of the importance of pressure in science, we can classify the application of this presented low-cost optical pressure sensor in general way as given below

(a) Medical field- We know that the small change in atmospheric pressure affects the human body to cause the neurological disorder. By using such type of sensors it is possible to know a very small change in atmospheric pressure in our surrounding environment that can be helpful in the situation of neurological disorder to prevent us from a disease like headaches, blood pressure problems.

(b) Industries – In many industrial sectors like gas refinery and oil refineries pressure change a very major role if any gas leakage is has happened, it creates the change in surrounding pressure of company area which can be detected by such type of sensor to protect the people from an explosion or fire.

(c) Others- In the various field of science and research like bioscience, chemical science, and optical science it can be used for various purposes.

2 PDMS Flexible Grating

PDMS flexible grating is designed by drawing the grating pattern on thin Polydimethylsiloxane (PDMS) film which is optically transparent and, in general, inert, non-toxic, and non-flammable polymer [18].

2.1 Polydimethylsiloxane (PDMS)

Polydimethylsiloxane is a member of a polymeric group known as organosilicon polymers which are commonly known as silicones [19-20]. It is famous for its various optical and other properties like optically clear, inert, non-toxic and non-flammable. It is one type of polymerized silicone and it has various applications in a field like medical, optical, microelectronics, elastomeric device and also in lubricant [21].

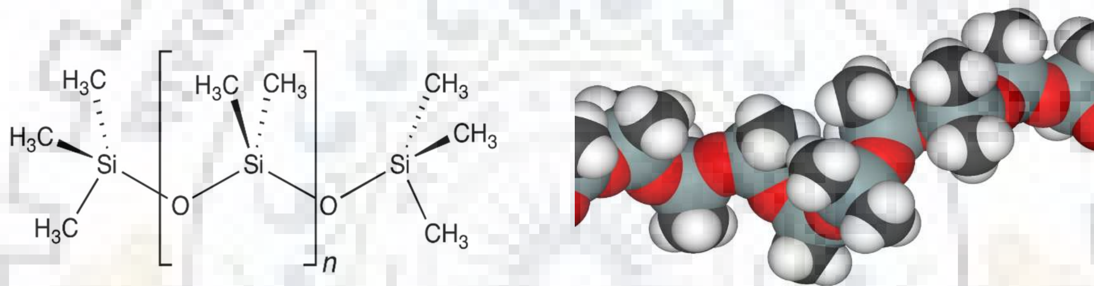

Fig- 1.6 (a) Chemical structure of PDMS and (b) 3D view of PDMS molecular chain [20]

We check the chemical combination or chemical formula of PDMS, we find that it is a chain like the structure of monomer unit $[SiO(CH_3)_2]$ [22]. On an industrial scale, it is synthesized from dimethyl-dichlorosilane and water by the following reaction

$$nSi(CH_3)_2Cl_2 + (n+1)H_2O = HO[-Si(CH_3)_2O-]_nH + 2nHCl \quad (1)$$

2.2 Mechanical Properties of PDMS

PDMS has various mechanical properties as it is vicious in nature just like honey at a higher temperature and act as elastic rubber [22]. Due to elastic nature, it can be easily stretched up to a certain limit after this it will return to its original state under its restoring limit or elastic limit beyond which it is broken just like rubber in nature. The surface structure of solid PDMS is converted into the hydrophobic surface structure after polymerization and cross-linking [23-24].

Normally the elastic modulus of polymers is their important properties which is determined by Hooke's law with the help of this we can calculate Young's Modulus Y as given below

$$Y = \frac{\sigma}{\varepsilon} \tag{2}$$

Where σ is the stress and ε is the strain that can be either tensile or compressive. Stress is the force per unit area and strain is the change per unit length [25-27].

For an ideal viscous liquid, Newton's law states the shear viscosity η which is given as below

$$\eta = \frac{\tau}{\frac{d\gamma}{dt}} \tag{3}$$

Tau indicates the shear stress and gamma indicates the shear strain and t is the time. The shear modulus of PDMS varies with preparation condition but typically in its range is 100 KPa to 3 MPa [28-29]. Equation (2) explain the mechanical behavior of ideal elastic solids and equation (3) predicts the ideal mechanical properties of ideal viscous liquids.

2.3 Diffraction Grating

In Optics and Photonics, the diffraction grating is a very important optic tool having periodic structure due to which the light gets diffracted in different directions and it splits the light in several light beams depending on the periodic structure and the wavelength of incident light [30]. The grating is also known as the dispersive element. Gratings are used in some important optical types of equipment like monochromators and spectrometers.

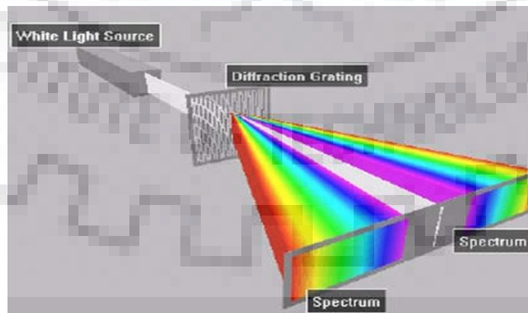

Fig-1.7- Normal grating spectrum [30]

2.4 Working principle of the Diffraction grating

For an ideal grating consisting of a set of slits having grating spacing d which is wider than the wavelength of interest to cause diffraction. Assuming a plane wavefront of wavelength λ incident normally on the grating where each slit in the grating acts quasi point light source to cause the light propagation in all possible directions [31]. When the path difference between the two light beams from adjacent slits is half of the incident wavelength, the wave will be out of phase to produce a point of minimum intensity if the path difference is equal to the incident light wavelength, the waves will be in phase to produce the point of maximum intensity [32].

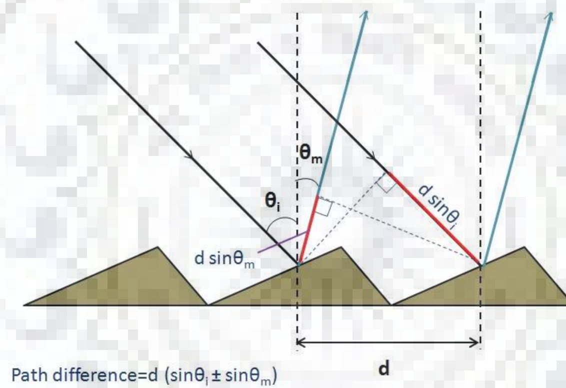

Fig-1.8 working principle of an ideal grating [31]

So the light maxima occur at angle θ_m that predicts the following relations

$$d sin\theta_m / \lambda = |m| \tag{4}$$

Where θ_m is the angle between the diffracted ray and the grating's normal vector, and *d* is the distance from the center of one slit to the center of the adjacent slot, and *m* is an integer representing the propagation-mode of interest.

It is straightforward to show that if a plane wave is an incident at any arbitrary angle θ_i, the grating equation becomes:

$$d(sin\theta_i - sin\theta_m) = m\lambda \tag{5}$$

The angle of diffracted maxima is given by

$$\theta_m = arcsin\left(sin\theta_i - \frac{m\lambda}{d}\right) \quad (6)$$

This equation is valid in the condition when both sides of the grating are in contact with the same medium as air (n=1).

3 Photodiode

A photodiode is a simple semiconductor device like a normal p-n junction diode. A photodiode is connected in reverse bias condition [33]. When the light photon having energy greater than and equal to the band gap energy of semiconductor material, it gets absorbed by the semiconductor material and electron-hole pair is generated resulting in the generation of photocurrent across the circuit [34].

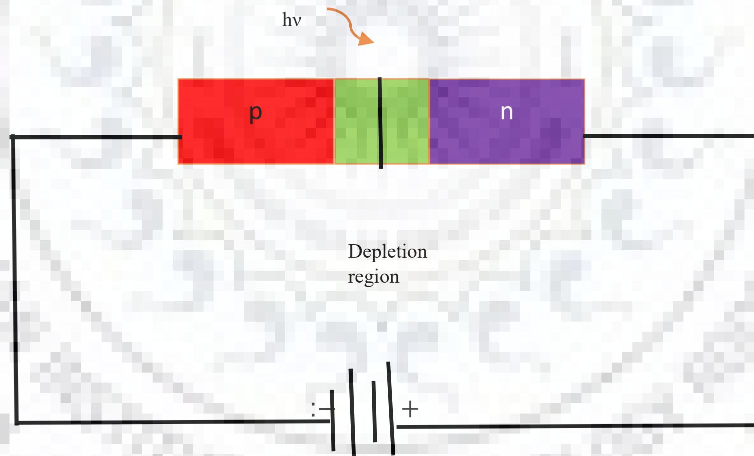

Fig-1.9 Schematic of normal Photodiode

Under the influence of applied voltage, electrons and holes swept across the semiconductor resulting photocurrent I_p which is directly proportional to the incident power

$$I_p = R_d P_{in} \quad (7)$$

Where R_d is the responsivity of a photodetector in(A/W) and P_{in} is the incident power [35].

3.1 Quantum Efficiency of Photodiode

The photodetector responsivity R_d can be expressed in terms of a fundamental quantity called quantum efficiency that is denoted by η and defined as following

$$\eta = \frac{Electron\ generation\ rate}{Photon\ incident\ rate} = \frac{h\nu}{q}\frac{I_p}{P_{in}} \quad (8)$$

$$\eta = \frac{h\nu}{q} R_d \quad (9)$$

$$R_d = \frac{\eta\,\lambda}{1.24} \quad (10)$$

The responsivity of a photodetector or photodiode increases with the wavelength λ simply because of the presence of more optical photon for the same optical power [36].

3.2 Hybrid Perovskite Photodiode

Here we are presenting a hybrid perovskite material based photodetector based on a thin single crystalline thin film (SC-TF) having thickness down to hundreds of nanometer range [37-39]. Single-crystalline perovskite-based devices including solar cells and photodetectors all have the active layers thicker than several micrometers. Due to its high absorption coefficient, perovskite materials can absorb the incident light completely in hundreds of nanometers [40]. Compared to the optimized film thickness in this range in devices based on polycrystalline films, the unnecessarily thick active layer in single crystalline perovskite-based devices leads to a longer transit time and a larger recombination probability for the photon excited carries, which degrades the device performance [41-43]. It is still very challenging to achieve simultaneously good crystallinity and proper thickness of perovskites in optoelectronic devices.

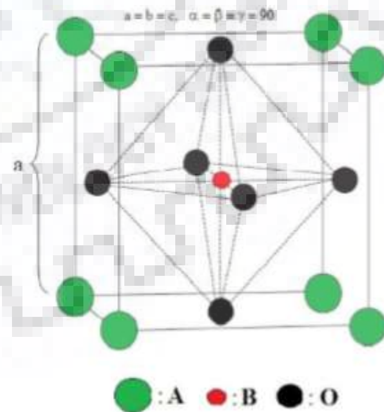

Fig-1.10 Schematic of perovskite crystal

3.3 Hybrid Perovskite Material

In the history of material science, first perovskite material is discovered in the Ural Mountains of Russia by Gustav Rose in 1839. It is named after a Russian nobleman and mineralogist Count Lev Aleksevich von Perovski (1792–1856) [44]. First Perovskite material was calcium titanium oxide (CaTiO3). Generally, Perovskites have the general formula ABX3. A and B are cations, X is the anion and also A being larger than B [45]. X is often oxygen but also other large ions such as halides, sulfides and nitrides are possible. Perovskite materials have an octahedral cubic structure. For hybrid halide perovskites of our present interest, the larger cation A constitutes the organic part which is used as generally Methylammonium ($CH_3NH_3^+$), Ethylammonium ($CH_3CH_2NH_3^+$).

Hybrid organic-inorganic perovskite material have attracted more and more the research community of material science or solar energy field since past six years due to its various versatile property as flexibility of energy band gap tuning, large area device fabrication and unparalleled growth rate of efficiency of photovoltaic devices like solar cells, light emitting diode (LED), photodiode or photodetector [45]. Such type of material is used for various applications as detectors, X-ray and gamma-ray detectors, field effect transistors [45]. Due to excellent light absorption and emission, high photo-luminescence, proper electron-hole diffusion length and long charge carrier lifetime these materials are used in various optoelectronic devices.

3.2 Tolerance Factor

The structural distortion in perovskite can be detected by the ratio of A and B ionic size and electronic configuration of the metal ions. The prediction criteria for identification of the formability of perovskite structure can be estimated by calculating tolerance factor (t') suggested by Goldschmidt as [45]. r_A and are r_B the ionic radii of the A and B cations and r_O is an ionic radius of oxygen anion

$$t' = \frac{(r_A + r_O)}{\sqrt{2}(r_B + r_O)} \quad (11)$$

For ideal cubic structure this factor 0.89<t<1 for oxide perovskite and 0.85<t<1.11 for halide perovskite, for t<0.85 octahedral tilting is expected [45].

CHAPTER-2

EXPERIMENTAL & CHARACTERIZATION TECHNIQUES

1. Scanning Electron Microscope (SEM)

First Scanning Electron Microscope was developed in the 1960s as the first commercial instrument. It is an efficient way to obtain images of the surface of a specimen. In this, the surface of a specimen is scanned with an electron beam in a raster pattern [46]. Using an electron beam instead of the light beam the magnified image of the surface of the specimen produced by SEM. The images created by light scanning are rendered black and white [47].

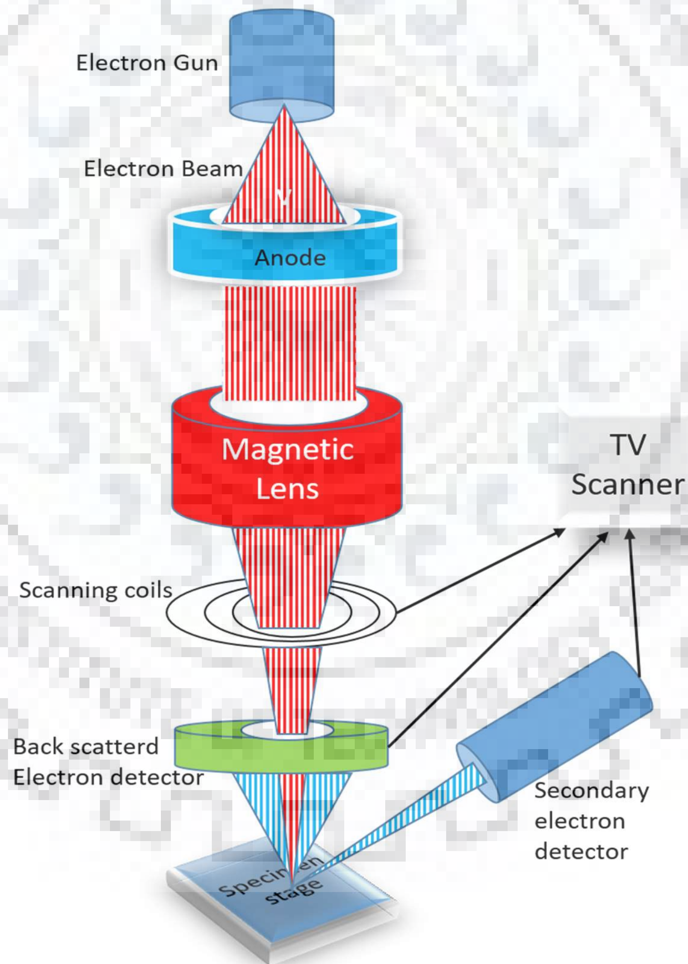

Fig-2.1 Schematic of SEM working

1.1 Principle of SEM

Accelerated electrons in an SEM carry a significant amount of kinetic energy and this energy is dissipated as a variety of signals produced by electron-sample interactions when the incident electrons are decelerated in the solid sample these signal include-

(a) Secondary Electrons (that produce SEM images)
(b) Backscattered electrons
(c) X-rays that are used for elemental analysis and crystallographic information
(d) Cathdoelumeniscence (Visible light)

Secondary electrons and backscattered electrons are commonly used for imaging samples [47]. These electrons are most valuable for showing morphology and topography on samples and backscattered electrons are most valuable for illustrating the contrast in composition in multiphase samples [47].

1.2 Applications of SEM

The SEM or FE-SEM is mainly used for the following purposes-

(a) To generate high-resolution images of shapes of objects and to show spatial variation in chemical composition.
(b) To identify phases of qualitative chemical analysis or crystalline structure.
(c) Precise measurement of very small features and objects down to 50nm in size.
(d) To examine microfabric and crystallography orientation in many materials.

2. Atomic Force Microscope (AFM)

The Atomic Force Microscope (AFM) is a very high-resolution type scanning probe microscopy technique with a domesticated revolution on the order of a fraction of a nano-meter, more than a 1000 times better than the optical diffraction limit [48]. The AFM was invented by Binnig, Quate, and Gerber in 1986 [48]. It is the foremost tools for imaging.

2.1 Working of AFM

The AFM consists of a cantilever with a probe at its end which is used to scan the surface of specimen or sample. The cantilever is made by the silicon material or silicon nitride material having the tip of the radius of curvature on the nano-meter order. When

this tip is brought into sample surface proximity force between the tip and the sample cause deflection of the cantilever following the Hook's law [49].

The cantilever deflection is measured using a laser spot reflected from the top of the cantilever into an array of the photodiode. The sample is mounted on a piezoelectric tube that can move the sample in the Z direction for maintaining a constant force, and the X and Y directions for scanning the sample topographic structure [49].

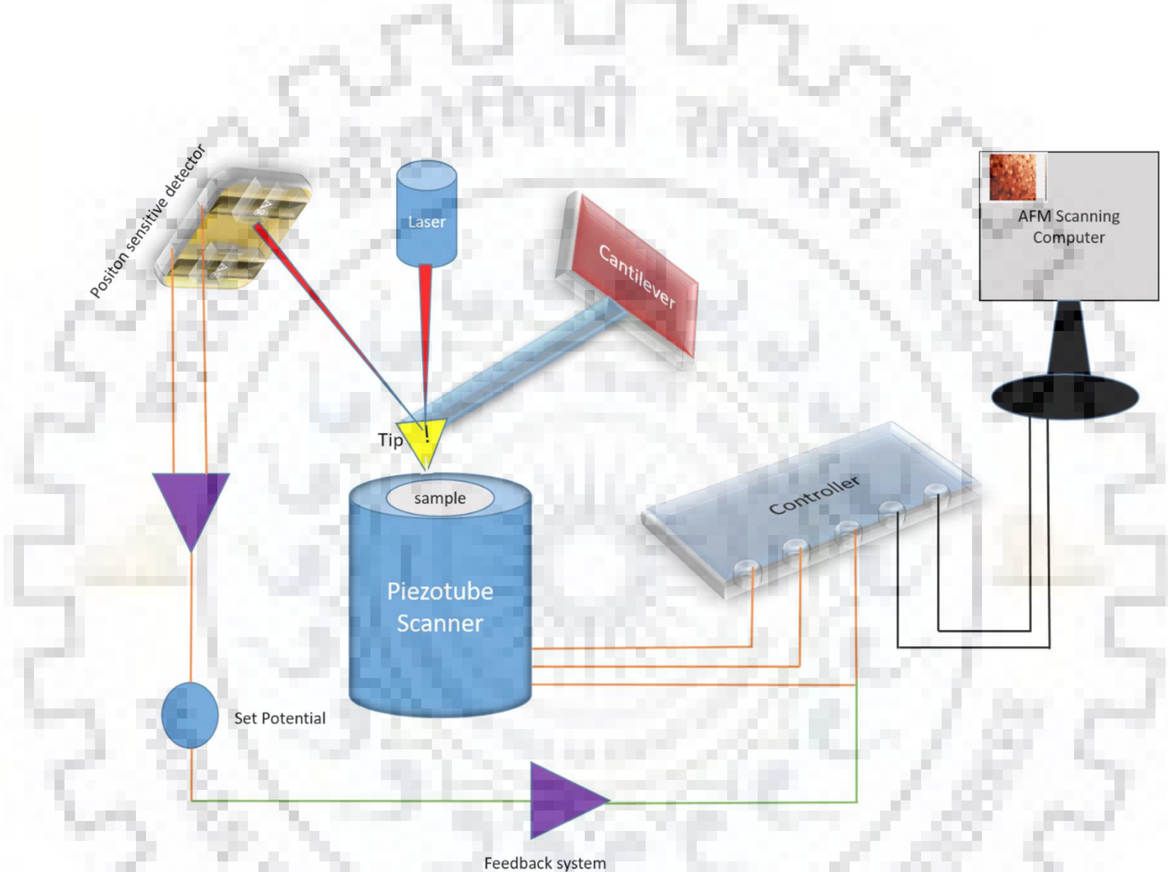

Fig-2.2 Schematic of AFM working

2.2 Application of AFM

Atomic Force Microscope is mainly used for the following imaging purpose-

(a) Semiconductor science and technology
(b) Thin film and coatings
(c) Tribology (surface and friction interactions)
(d) Surface chemistry
(e) Polymer chemistry and physics
(f) Cell biology

(g) Molecular biology

(h) Energy storage (a batter) and energy generation (photovoltaic) materials

(i) Piezoelectric and ferroelectric materials

3. Spin Coating

Spin coating is an experimental technique that is used to deposit a thin film on a floated substrate which is mounted in spin coater by applying vacuum. Thickness of the coated film is controlled by rotation per minute (RPM), rotation acceleration, rotation time within the limit from nanoscale to microscale and the viscosity of the chemical or the solution which is to be deposited on the mounting substrate also affect the thickness of the thin film deposited by the spin coater [50].

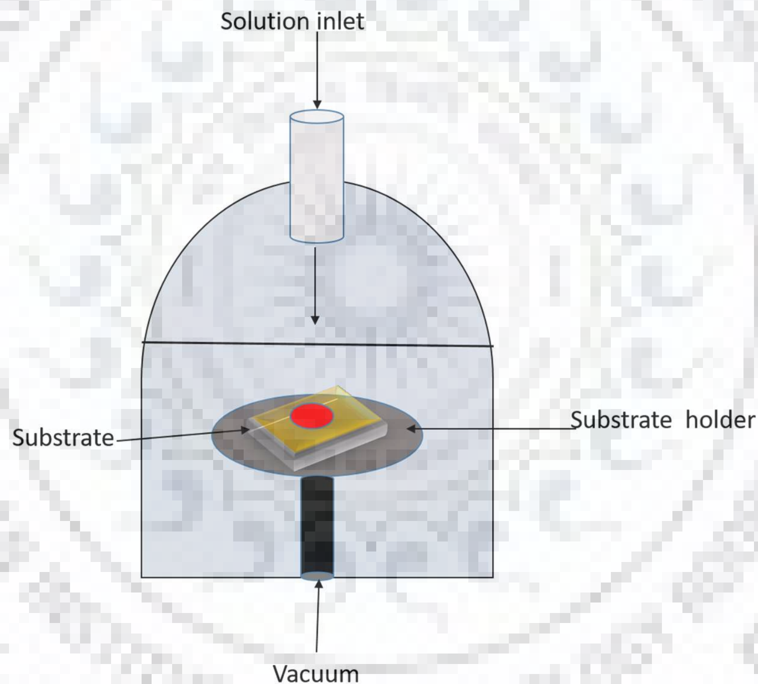

Fig-2.3 Schematic of Spin coater working

CHAPTER-3

TRANSDUCER

(Pressure Sensing Using PDMS Flexible Grating)

1 Flexible PDMS Grating

Due to its novel various properties PDMS is used in various scientific research field like microelectronics, human robotics, touch interfaces, flexible pressure sensor due to its flexible nature in the form of key components for the next generation of sensor technology and flexible electronics. Using its flexible nature we have designed flexible grating to use a deflection diaphragm in our proposed low cost optical pressure sensor

1.1 Methodology for PDMS Grating

We have used soft lithography technique to fabricate flexible PDMS grating. Most widely used PDMS network 10:1 is followed for thin PDMS film and 10:1 means that ten part of mass of silicon elastomer as base with 1 part of mass silicone elastomer curing regent for PDMS solution.

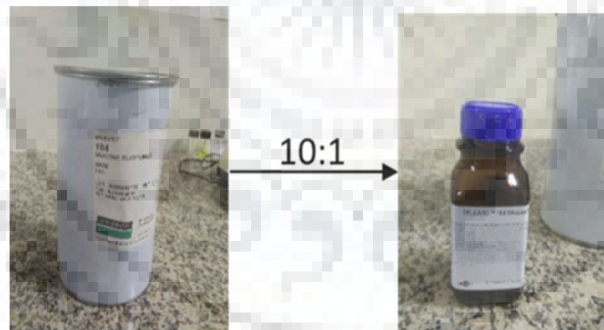

Fig-3.1 Silicone elastomer base and its curing regent

Thickness of PDMS film has very versatile roll in presented low cost optical pressure sensor because the thickness of PDMS film will controlled the range of applied pressure or sensitivity of the pressure sensor. To achieve more thin film like 5µm we have to use tert-butyl alcohol (TBA) and hexane but to dilute more PDMS is used and film thickness for different concentration of PDMS in TBA as function of speed spin coating as explained in literature []. Following that reference we have designed 70µm thin film of PDMS using 500 rpm coting speed and 3 minute spin time for 100% PDMS concentration. To find the grating structure on

thin PDMS film we have chosen compact disk (CD) pattern. Silver coating is removed from the CD using paper tape technique. Different pieces of CD are dipped in Iso-Propyl Alcohol (IPA) for different time as 20min, 30min, 40min, 50min, 60min to remove the chemical coating from the CD.

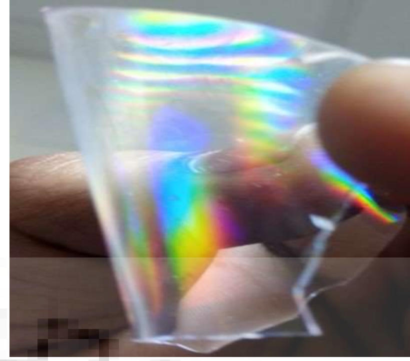

Fig-3.2 Picture of flexible PDMS Grating

Following thisprocedure base stamp are achieved to transfer the grating pattern from CD to PDMS film. To transfer the grating pattern PDMS is spin coated on the base stamp using the above mentioned spin coating spin parameters. Coated samples are cured using hot plate for 3 hour at 100°C temperature to crosslink. After this whole procedure thin film of PDMS having grating structure is removed from CD using paper tap.

2. Characterization of PDMS Grating

To check the gating pattern, its grating pitch and its grating depth we have used Atomic Force Microscope (AFM) technique by which grating depth profile and its pitch can be determined with the help of given below AFM results

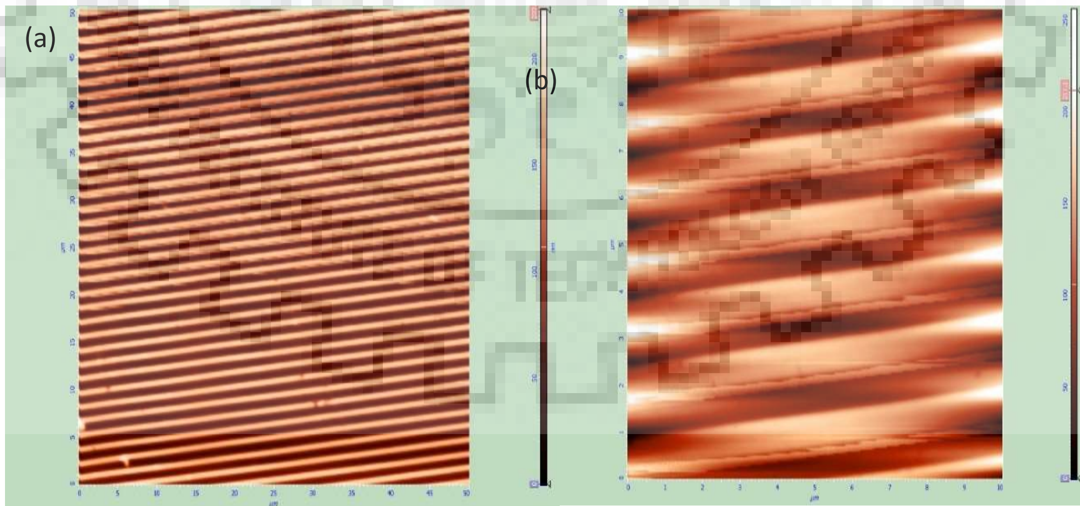

Fig-3.3 For 20 minute in IP dip CD (a) and (b)AFM 2D view of grating surface (c) Line profile of grating surface depicting average depth 160 nm and grating pitch 1.4 µm

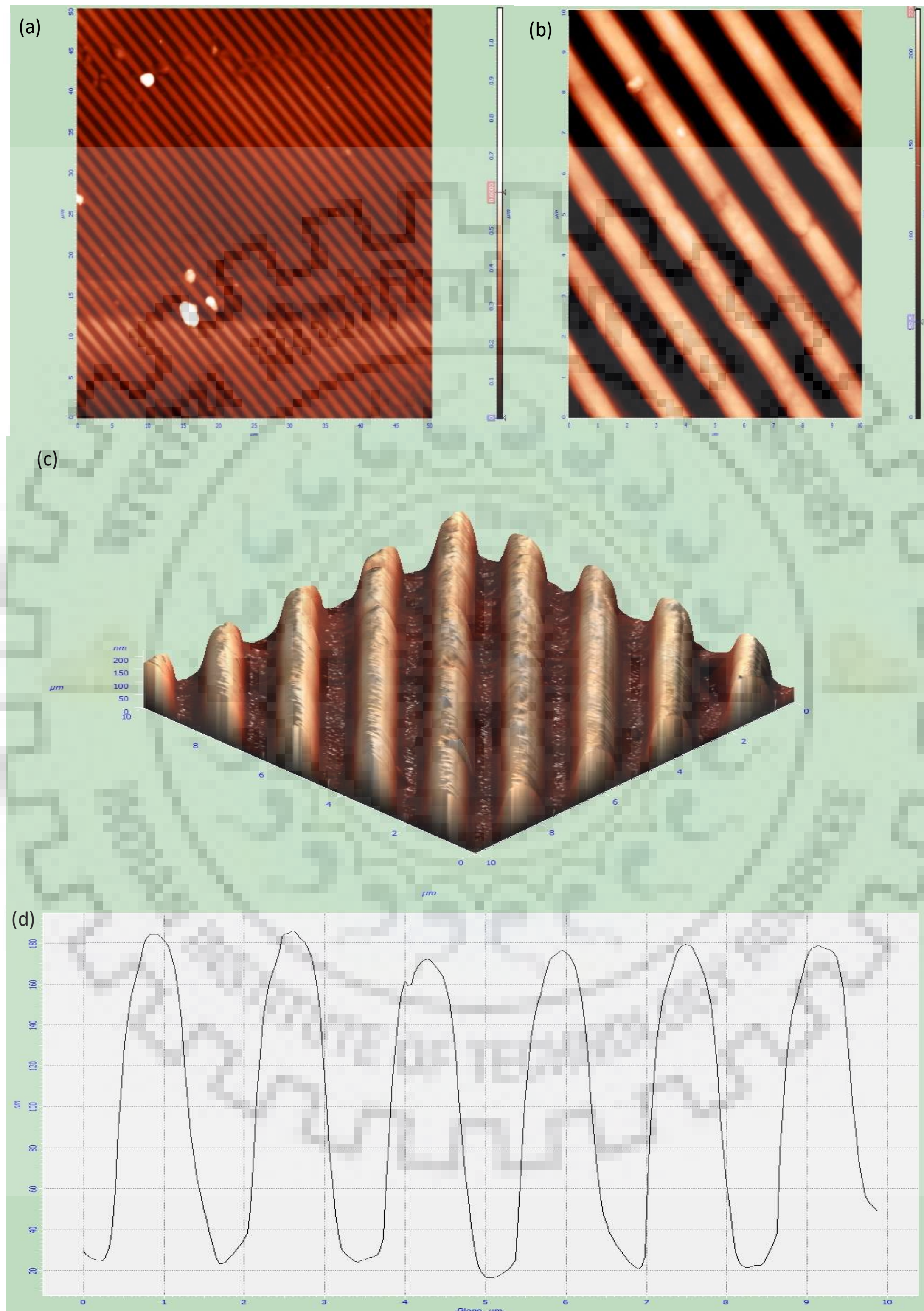

Fig-3.4 For 30 minute in IP dip CD(a)AFM 2D view of grating surface for 50μm square scanning area(b) AFM 2D view of grating surface for 10μm square scanning area (c) AFM 3D view of grating surface and (d) Line profile of grating surface depicting average depth 160 nm and grating pitch 1.4 μm

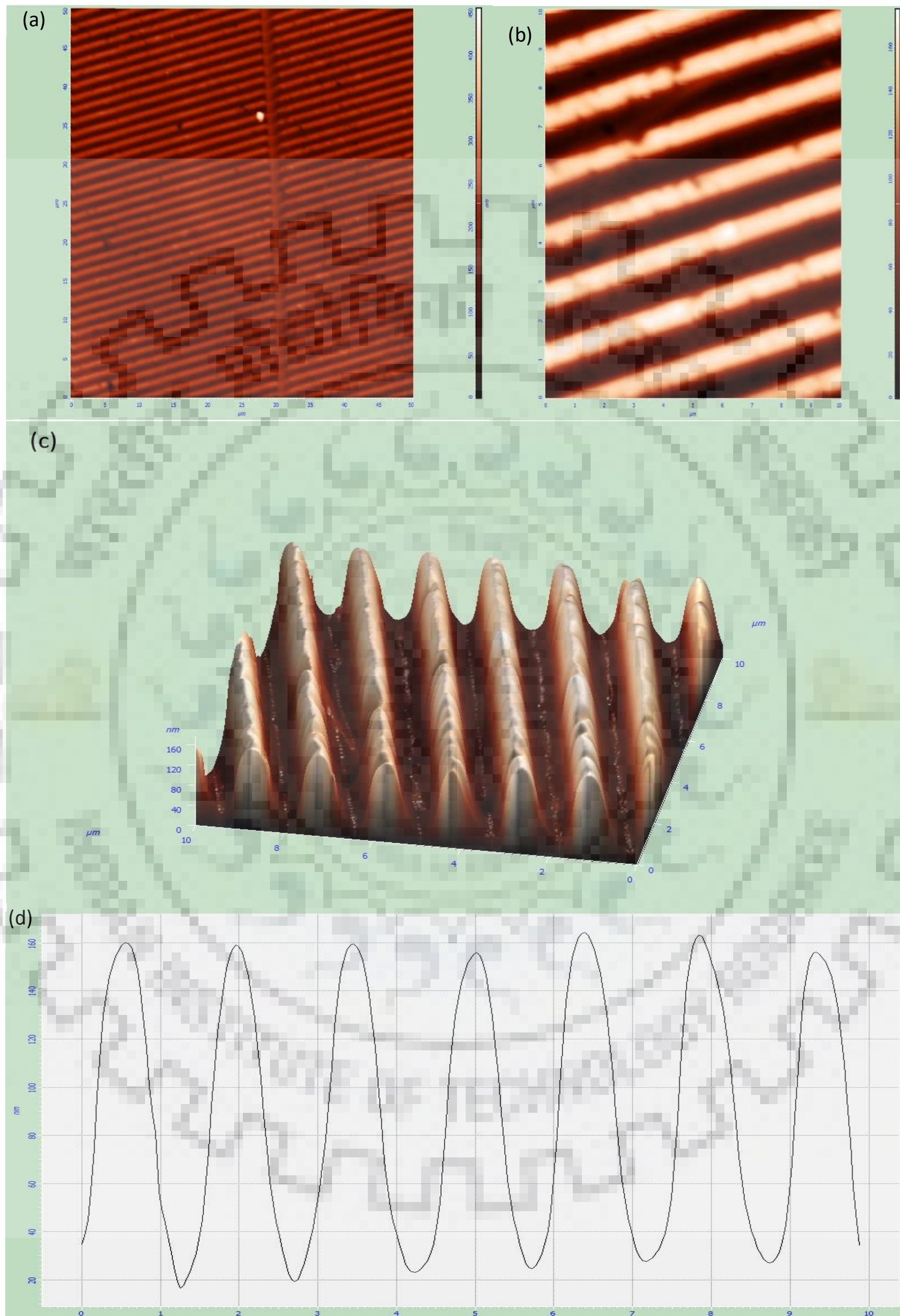

Fig-3.5 For 40 min in IP dip CD (a)AFM 2D view of grating surface for 50µm square scanning area(b) AFM 2D view of grating surface for 10µm square scanning area (c) AFM 3D view of grating surface and (d) Line profile of grating surface depicting average depth 160 nm and grating pitch 1.4 µm

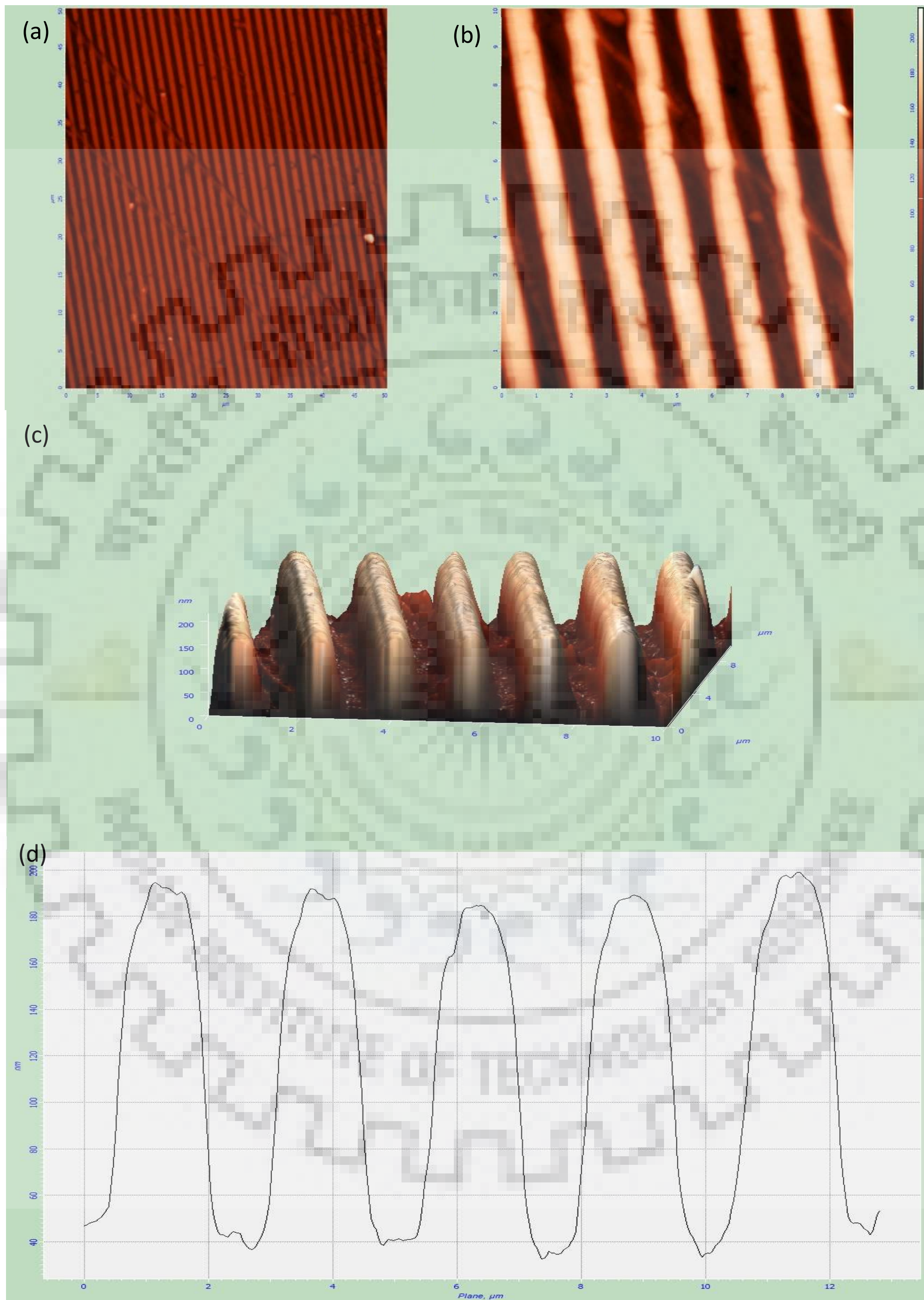

Fig-3.6- For 50 minute in IP dip CD (a)AFM 2D view of grating surface for 50µm square scanning area(b) AFM 2D view of grating surface for 10µm square scanning area (c) AFM 3D view of grating surface and (d) Line profile of grating surface depicting average depth 160 nm and grating pitch 1.4 µm

Fig-3.7- For 60 min in IP dip CD (a)AFM 2D view of grating surface for 50µm square scanning area(b) AFM 2D view of grating surface for 10µm square scanning area (c) AFM 3D view of grating surface and (d) Line profile of grating surface depicting average depth 160 nm and grating pitch 1.4 µm

For DVD pattern

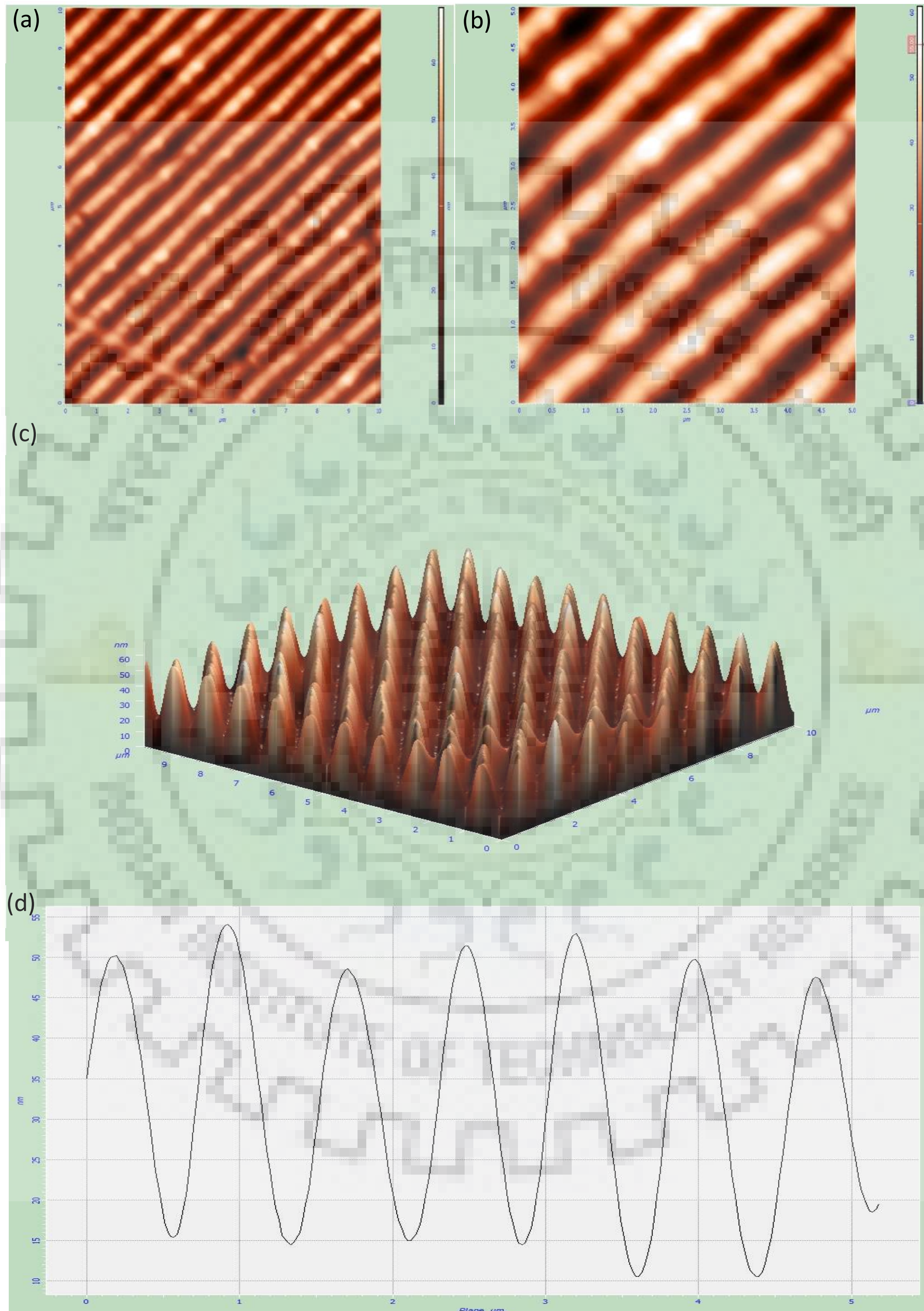

Fig-3.8- for DVD pattern (a)AFM 2D view of grating surface for 10µm square scanning area(b) AFM 2D view of grating surface for 5µm square scanning area (c) AFM 3D view of grating surface and (d) Line profile of grating surface depicting average depth 50 nm and grating pitch 0.7 µm

3 Optical Characterization of PDMS Grating

Our aim to design flexible PDMS grating is to use as deflection diaphragm in our purposed low cost optical pressure sensor. As much as pressure will be applied on the centre of PDMS grating its grating pitch will change and the monochromatic light makes an incidence on the PDMS grating will be diffracted. To check optical behaviour of the grating we should have an idea of modulus of elasticity of PDMS grating because PDMS is elastic material like rubber. Elastic properties of PDMS film depends on the ratio of Sylgard 184 silicone elastomer base and silicone elastomer curing agent according to formula []

$$Y = \frac{20MPa}{n} \quad (1)$$

Where Y is the modulus of elasticity of PDMS film and n is the ratio of Sylgard 184 silicone elastomer base and silicone elastomer curing agent.As reported by one research group from University of South Florida in 2011 is that elastic modulus of 10:1 network of PDMS is 2.63MPa and 5:1 network sample of PDMS elastic modulus is 3.584MPa []. 10:1 network of PDMS film is used for this low cost optical pressure sensor so the elastic modulus of our flexible PDMS grating may be considered as 2.63MPa. Following arrangement is used to record the response of PDMS grating with different light source with different light source.

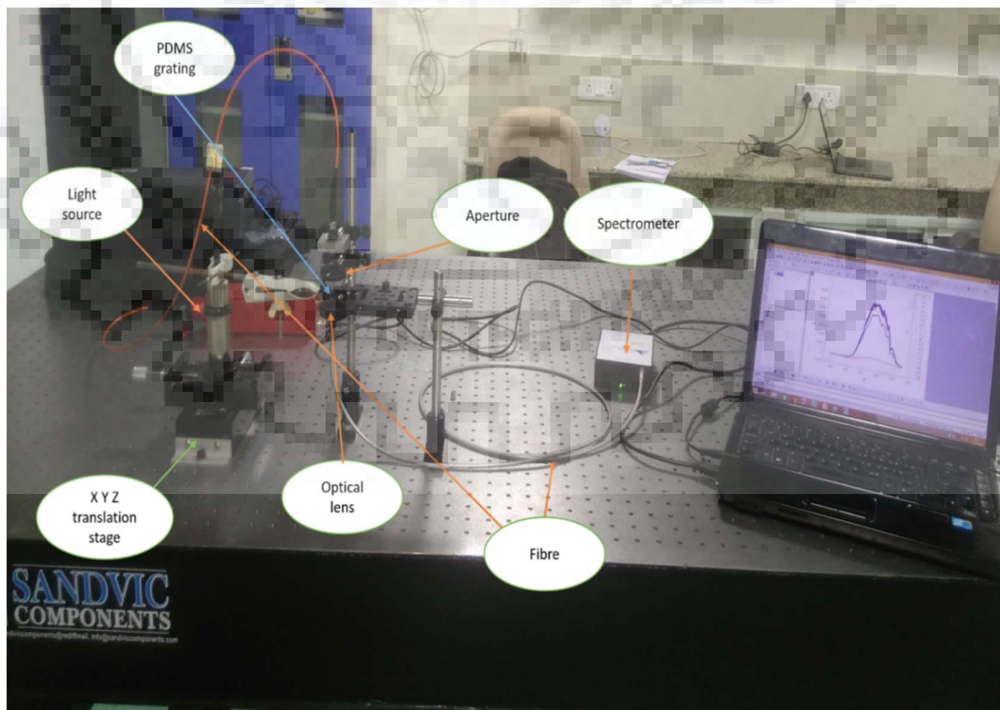

Fig-3.9 (a)

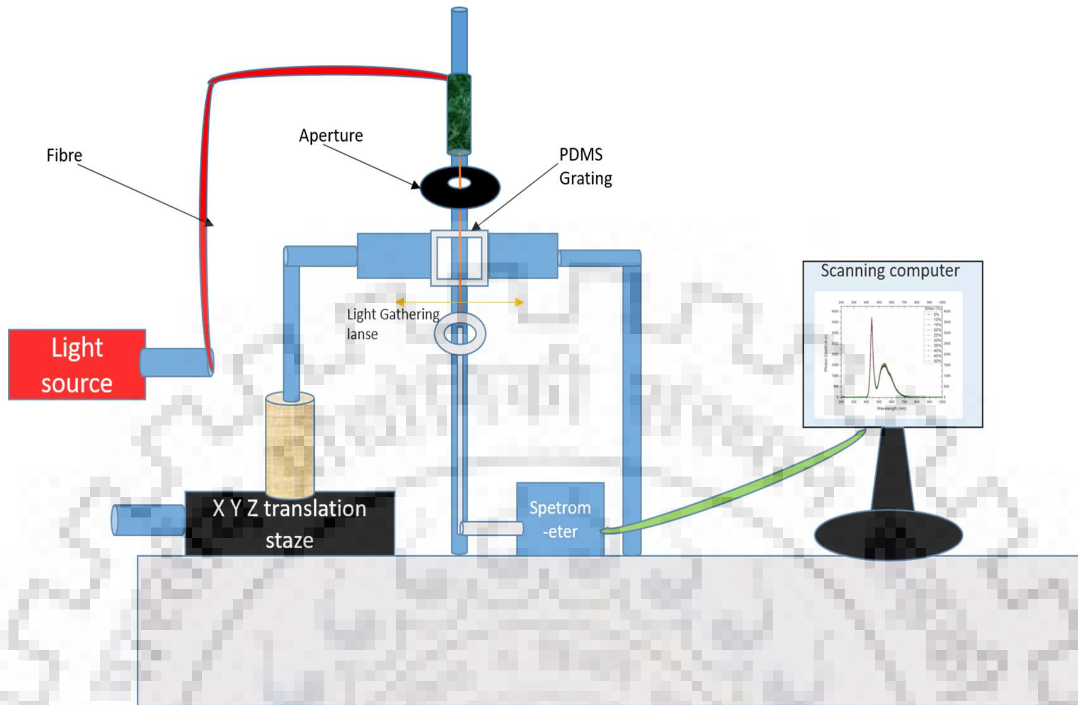

Fig-3.9 (b)

Fig-3.9 Optical arrangement to record the response of PDMS grating for different light source with stretching of grating.

4 Grating Height variation with dip time in IPA

We have designed the PDMS gratings having grating pitch 0.7 µm by dipping the different CD base in iso-propyl alcohol to get ready the pattern mask for different time as following

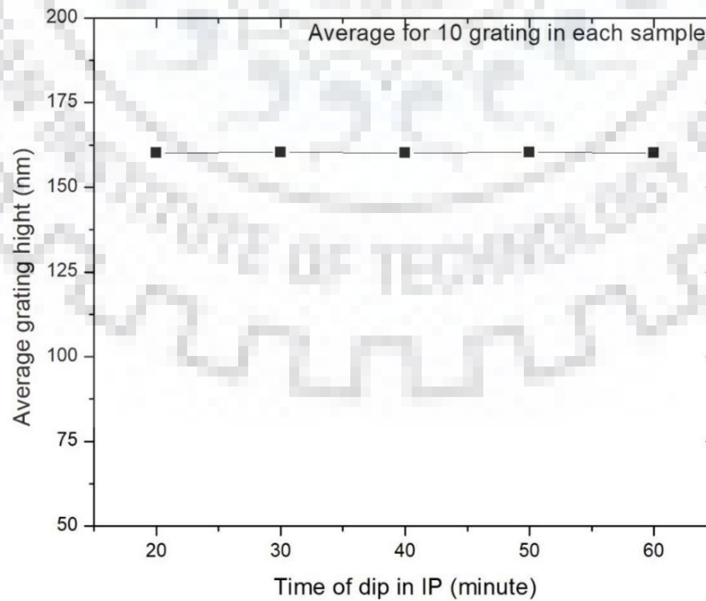

Fig-3.10 Grating height V/s IPA dipping time

We have selected 10 grating sample to calculate the average height of grating for each sample of grating and it is concluded that the average height of grating in each PDMS sample is 160nm.

5 Calculation for Longitudinal Pressure

We are using flexible grating as deflection diaphragm in presented low cost optical pressure sensor. When pressure will be applied on the diaphragm it acts as longitudinal pressure and induced the force at the centre of diaphragm to change the grating pitch of PDMS grating. So if we have idea about the strain induced in grating pitch we can calculate how much pressure should be applied on the diaphragm to find the better sensitivity of the presented low cost optical pressure sensor and it can be calculated as given below

Modulus of elasticity of PDMS grating is

$$Y = \frac{\text{Stress}}{\text{Strain}} \tag{2}$$

$$\text{Stress} = \frac{F}{A} = \text{Longitudinal force per unit area}$$

$$= \triangle \mathbf{P} \tag{3}$$

As mentioned above the modulus of elasticity of 10:1 network of PDMS film is 2.63MPa will be used for our flexible PDMS grating having 100µm thickness

5.1 Calculation for Strain in PDMS Grating

In one rotation of Vernier scale it covers 0.5mm distance because lest count of Vernier scale in XYZ translation stage is 0.005.

In case of CD pattern area of selected PDMS flexible grating for observation is 1cm square

$$A = 1cm^2 \tag{4}$$

Length of grating is 1cm but the width or pitch of grating in case of CD pattern is 1.4micrometer so the area covered by one grating is

$$a = 1cm \times 1.4\mu m \tag{5}$$

Total number of grating in 1cm square area are

$$N = \frac{A}{a}$$

$$=7142.857 \quad (6)$$

After one rotation of Vernier scale length of grating is increased by 0.5mm so the new area of grating is

$$A_2 = 1.05cm^2 \quad (7)$$

And the new area covered by grating

$$a_2 = 1cm \times X\mu m \quad (8)$$

Because number of gratings is constant for selected area of grating so N will remain same

Now $$N = \frac{A_2}{a_2}$$

$$X=1.47\mu m$$

It means after one rotation of Vernier scale grating pitch is increased from 1.4 to 1.47μm

So the strain induced in PDMS grating is

$$S = \frac{\Delta L}{L} = 0.05 \quad (9)$$

$$=5\%$$

Similarly, the strain induced in case of DVD pattern is 4.285%

5.2 Observation of Strain

Light response for PDMS flexible grating having CD pattern or grating pitch 1.4μm, using the above shown optical arrangement such type of grating behaviour is recorded

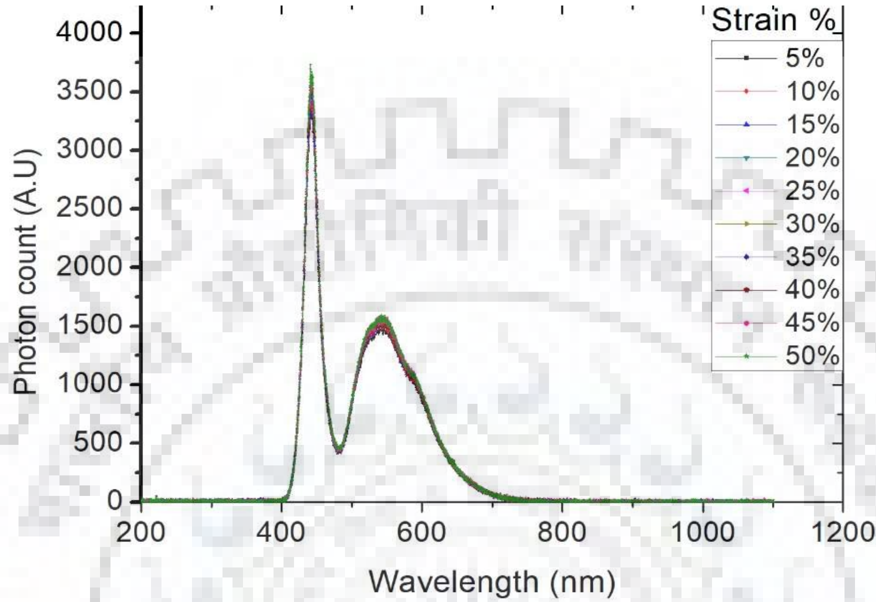

Fig-3.11 Photon count or density variation with strain induced in grating having 1.4 μm grating pitch

If we chose a particular wavelength for highest peak in spectrum as 427 nm or 541 nm and plot it with the strain

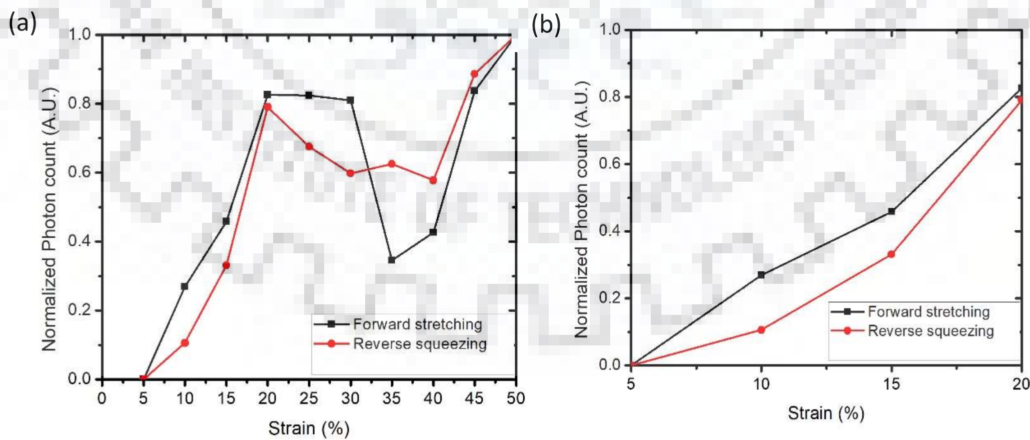

Fig-3.12 (a) and (b) is for particular wavelength for highest peak in spectrum as 541 nm and plot it with the strain in photon density mode.

In transmittance mode

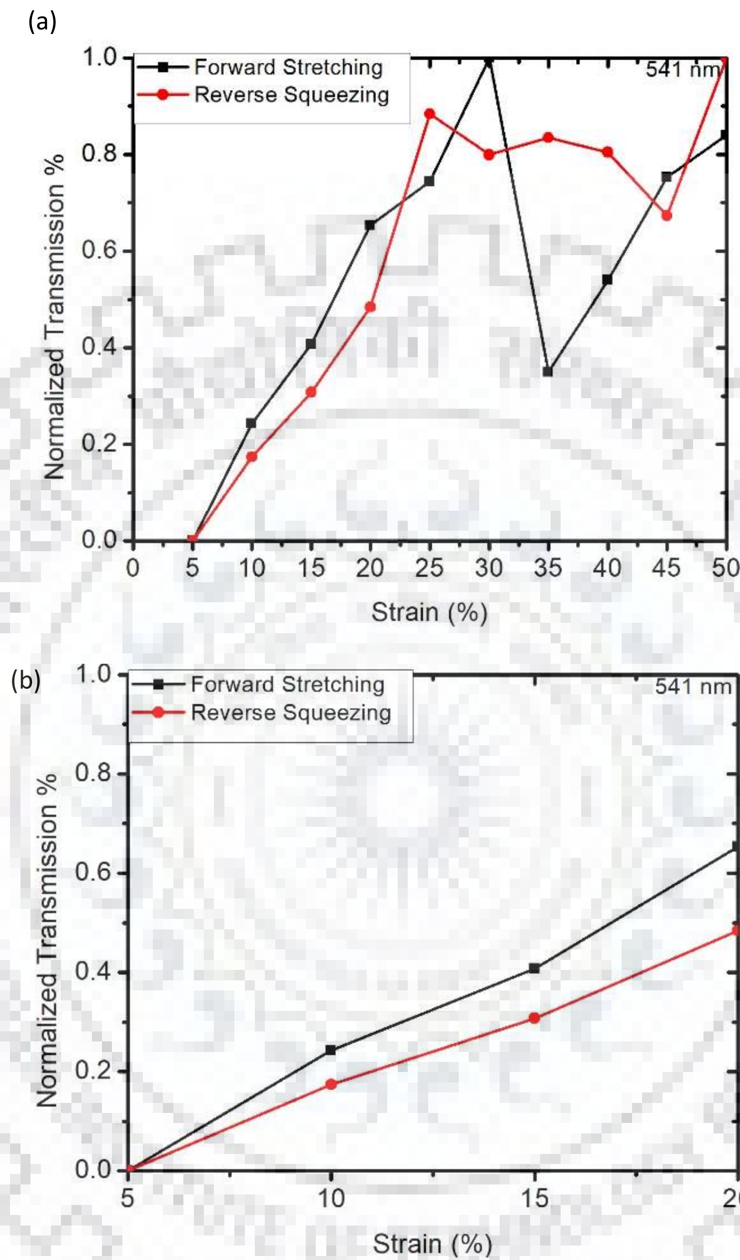

Fig-3.13 (a) and (b) is for particular wavelength as 541 nm and plot it with the strain in transmission mode.

It is verified with the graph of light response with strain induced in PDMS grating of 1.4 μm grating pitch in photon density or transmittance mode from 5% to 20% strain stretching and squeezing of PDMS grating it works in reliable mode.

Light response for PDMS flexible grating having DVD pattern or having grating pitch 0.7μm.

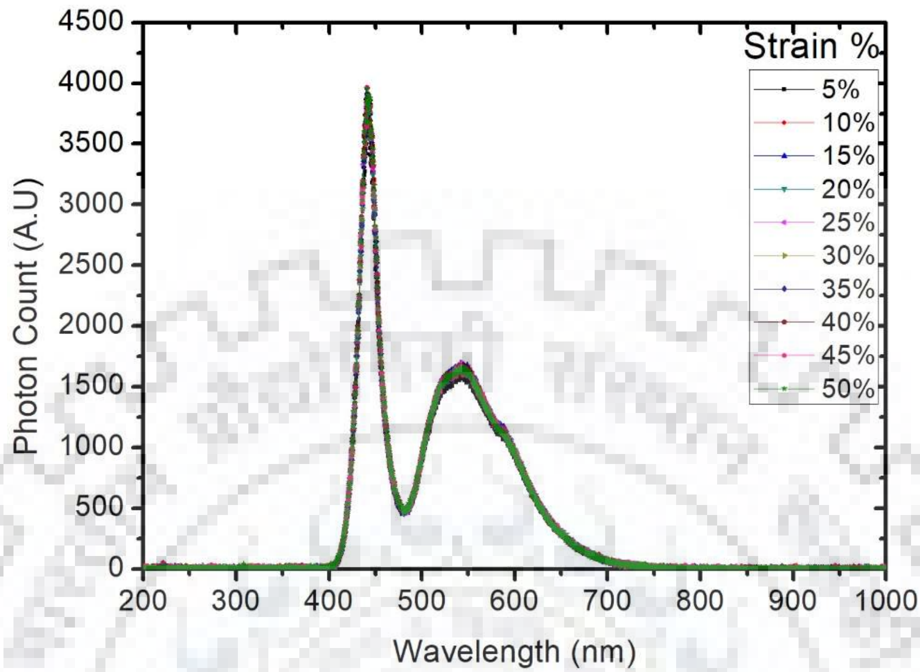

Fig-3.14 Photon intensity or density variation with strain induced in grating having 0.7μm grating pitch

If we chose a particular wavelength for highest peak in spectrum as 427 nm or 541 nm and plot it with the strain

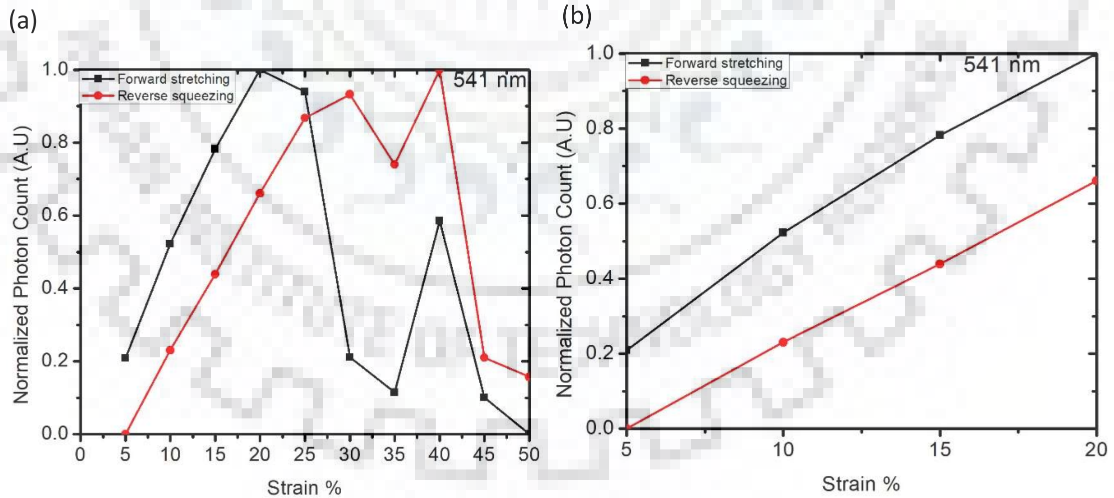

Fig-3.15 (a) and (b) is for particular wavelength for highest peak in spectrum as 541 nm and plot it with the strain in photon density mode.

In transmittance mode

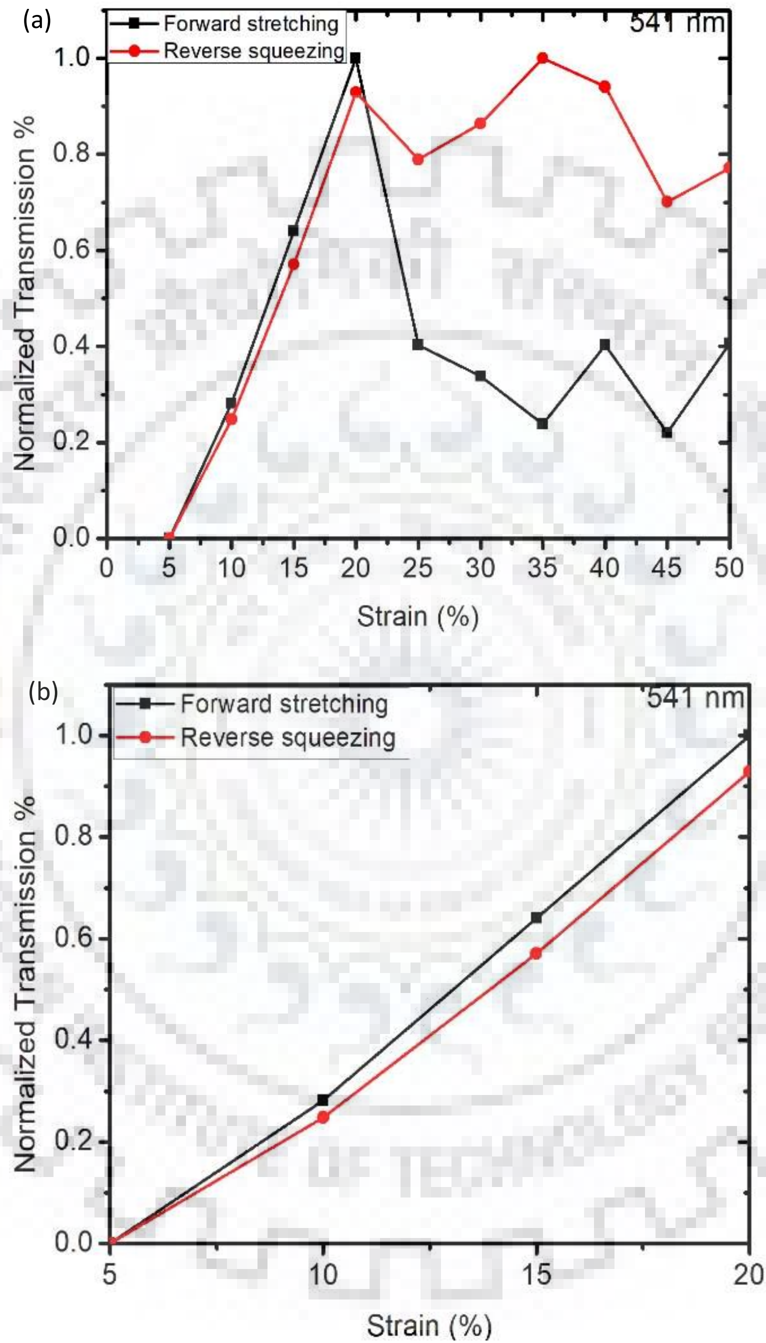

Fig-3.16 (a) and (b) is for particular wavelength as 541 nm and plot it with the strain in transmission mode

It is verified with the graph of light response in photon density or transmittance mode from 5% to 20% strain stretching and squeezing of PDMS grating it works in reliable mode.

Light response for simple PDMS film for same film thickness

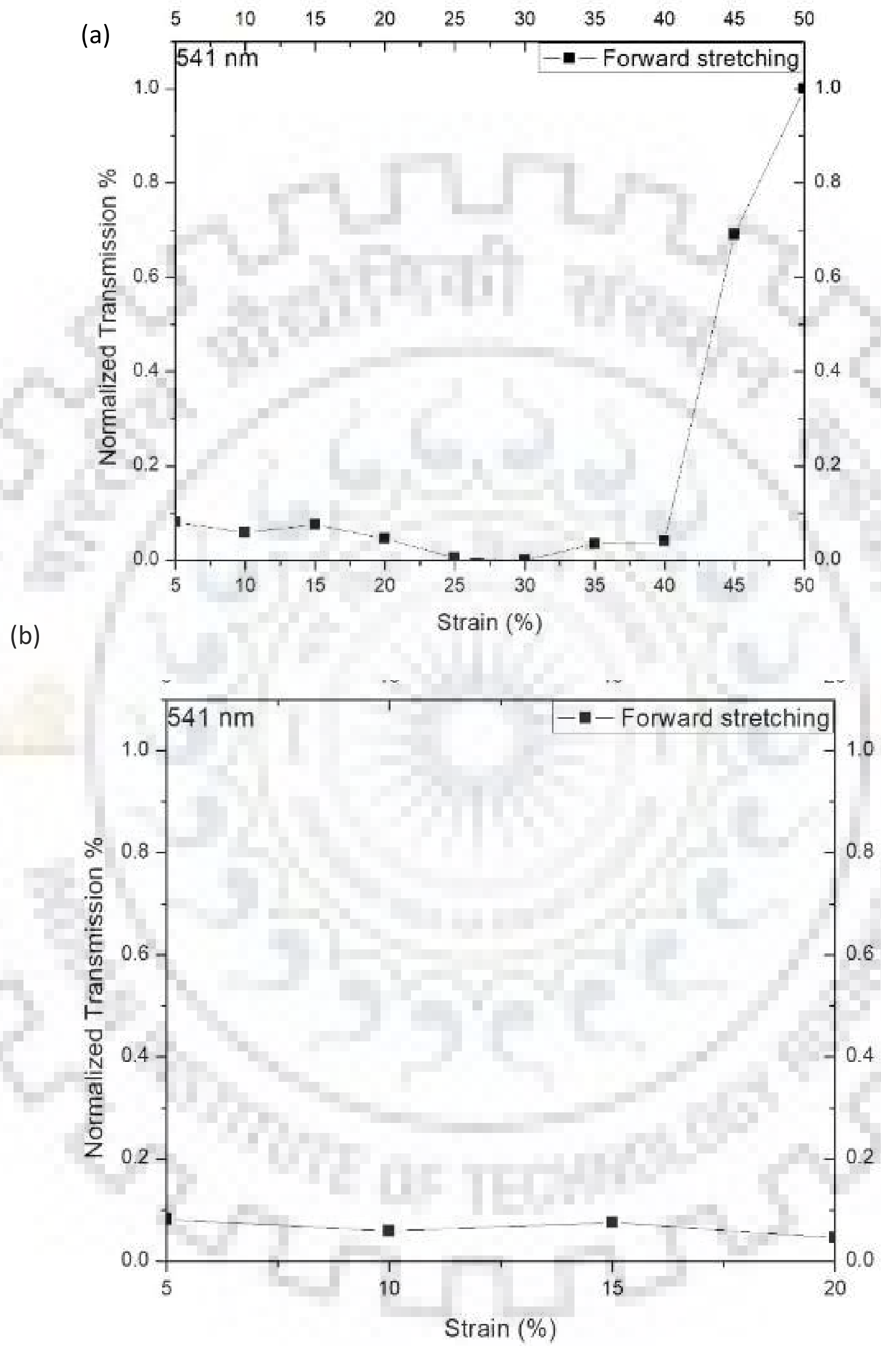

Fig-3.17 (a), (b) are for particular wavelength as 541 nm and plot it with the strain in transmission mode for simple PDMS film

5.3 Calculation for Pressure on PDMS Grating

5.3.1 For 1.4 µm Grating Pitch

It is predicted from the line graph for PDMS grating having *1.4 µm* grating pitch from 5% to 20% strain in grating photon intensity and transmittance increase and decrease almost similarly in stretching and squeezing mode respectively. If we make it from 5% to 20% or for 15% strain in PDMS.

As reported previously the modulus of elasticity of 10:1 network of PDMS film is 2.63MPa. Using the above mentioned relation for strain induced in PDMS grating and the modulus of elasticity of PDMS film range of applied pressure can be calculated in reliable range as given below

$$Y = \frac{\triangle P}{\text{Strain}} \quad (10)$$

Strain	Strain %	Pressure(MPa)
0.05	5	0.1315
0.10	10	0.263
0.15	15	0.3945
0.20	20	0.526

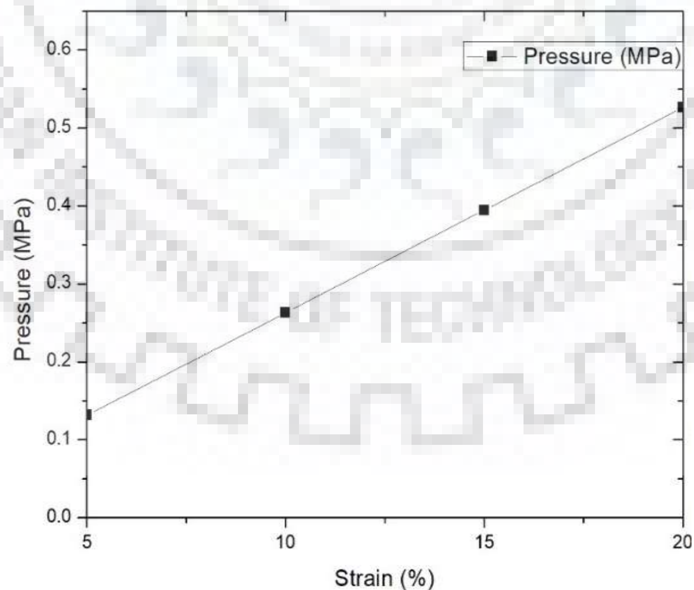

Fig-3.18 Variation in pressure with the increase in induced strain in PDMS grating of pitch 1.4 µm.

If we make it normalize from 5% to 20% or for 15% strain in PDMS, it can be calculated in such a way as

Strain	Strain %	Pressure(MPa)
0.0	0	0.0
0.05	5	0.1315
0.10	10	0.263
0.15	15	0.3945

For this calculation

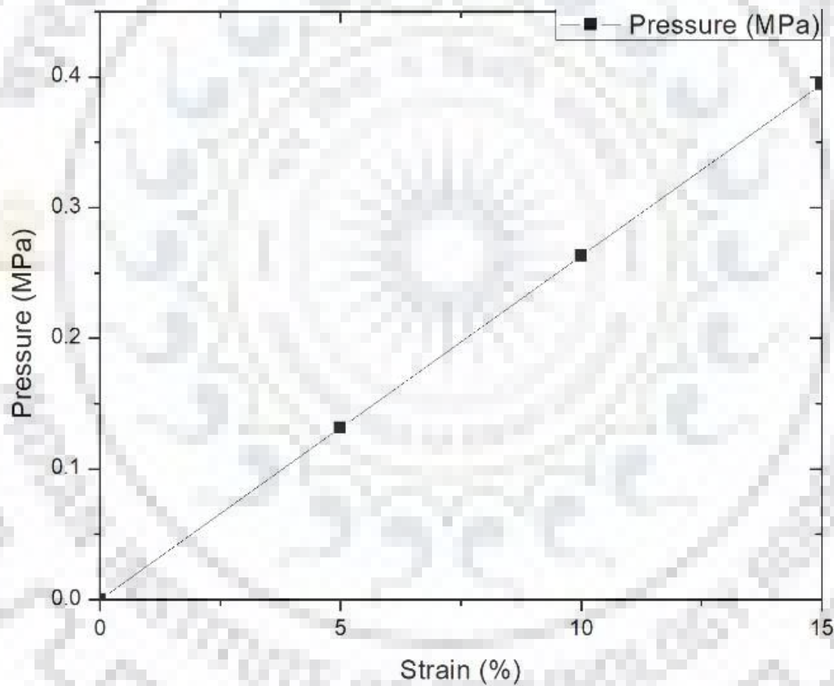

Fig-3.19 Change in pressure with change in induced strain in PDMS grating for 0% to 15% change in strain for grating pitch 1.4 μm.

This graph states that the range of applied pressure on the PDMS grating having 1.4 μm grating pitch working as deflection diaphragm is calculated as below

- Applied pressure range =0 to 0.3945MPa
- Sensitivity =0.0263MPa^{-1}

5.3.2 For 0.7 µm Grating Pitch

It is clear from the line graph for PDMS grating having *0.7 µm* grating pitch from 4.28% to 17.12% strain in grating photon intensity and transmittance increase and decrease almost similarly in stretching and squeezing mode respectively. If we make it from 4.28% to 17.12% or for 12.84% strain in PDMS. Using equation -12 the range of applied pressure on the PDMS grating is calculated as

Strain	Strain %	Pressure(MPa)
0.0428	4.28	0.112564
0.0856	8.56	0.225128
0.1284	12.84	0.337692
0.1712	17.12	0.450256

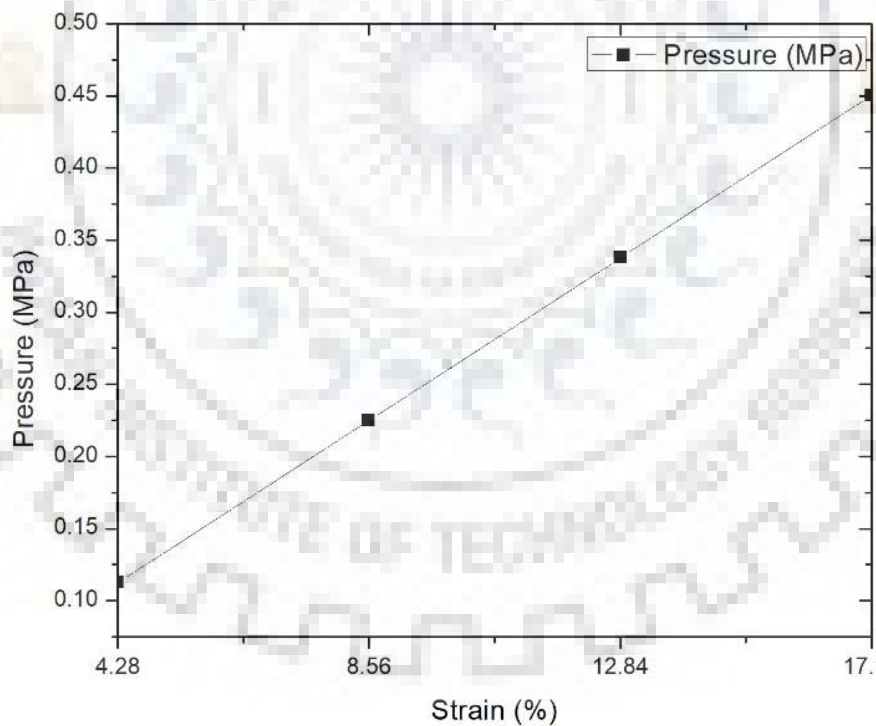

Fig-3.20 Variation in pressure with the change in induced strain in PDMS film for grating pitch 0.7 µm

If we make it normalize from 4.28% to 17.12% or for 12.84% strain in PDMS grating

Strain	Strain %	Pressure(MPa)
0.0	0	0.0
0.0428	4.28	0.112564
0.0856	8.56	0.225128
0.1284	12.84	0.337692

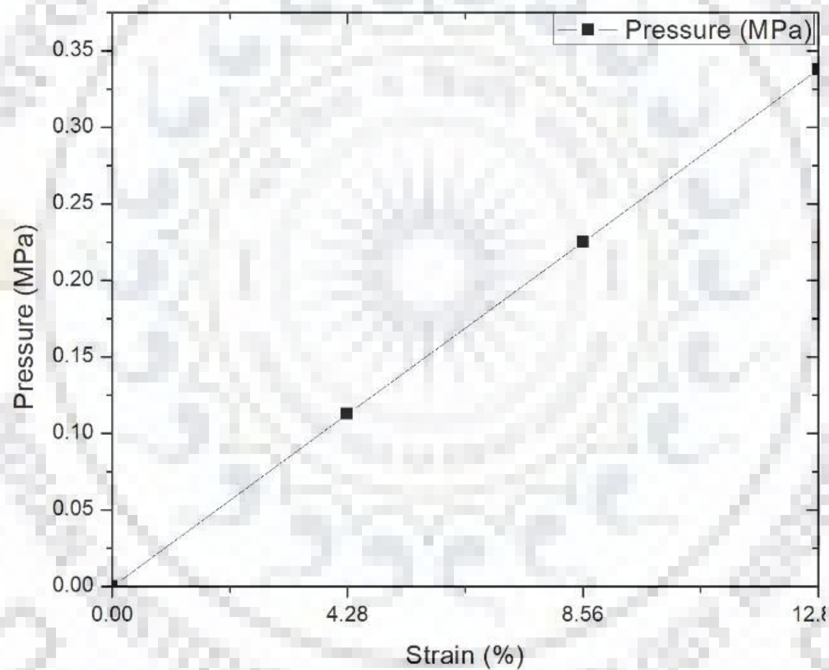

Fig-3.21 Variation in pressure with change in induced strain in PDMS grating for 0% to 13% change in strain for grating pitch 0.7µm.

Applied pressure range =0 to 0.337692MPa

Sensitivity =0.0263MPa^{-1}

In case of Simple PDMS film approximately there is no change in Photon intensity and transmittance of light with strain which is predicted by the line graphs in figure 5.8.

CHAPTER-4

DETECTOR

(Photocurrent Sensing by Hybrid Perovskite Photodiode)

1.Schematic of Perovskite Photodiode

We have used Methyl-ammonium lead bromide ($CH3NH3PbBr_3$) hybrid perovskite for thin film deposition to act as active medium in hybrid perovskite photodetector. Methyl-ammonium lead bromide is direct band semiconductor and ambi-polar charge transport material [8].

We have followed three different schematic geometry of perovskite photodetector to use it as signal detection component in our purposed low cost optical pressure sensor to check which geometry will give the better performance in the form photocurrent

(a) $ITO/MAPbBr_3/Ag$

(b) $ITO/PEDOT:PSS/MAPbBr_3/Ag$

(c) $FTO/TiO_2/MAPbBr_3/Ag$

(d) $FTO/TiO_2/MAPbBr_3/P3HT/Ag$

2. Energy band diagram of Perovskite Photodiode

We have followed the three different schematic geometry for the design of perovskite photodetector as mentioned above two of them (a) and (b) have p-i-n d photodiode structure and (c) and (d) have n-i-p photodiode structure. Each geometry will have different own energy band diagram with different charge transport nature as shown below

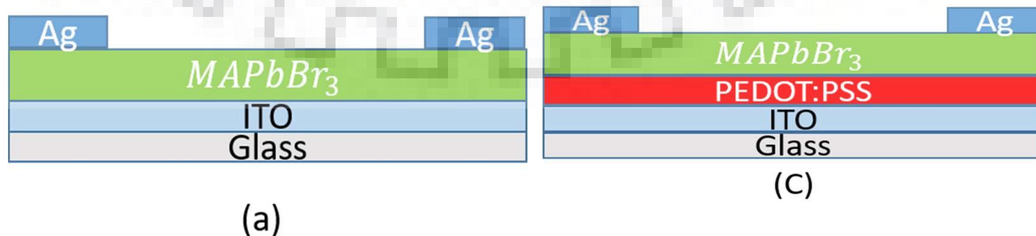

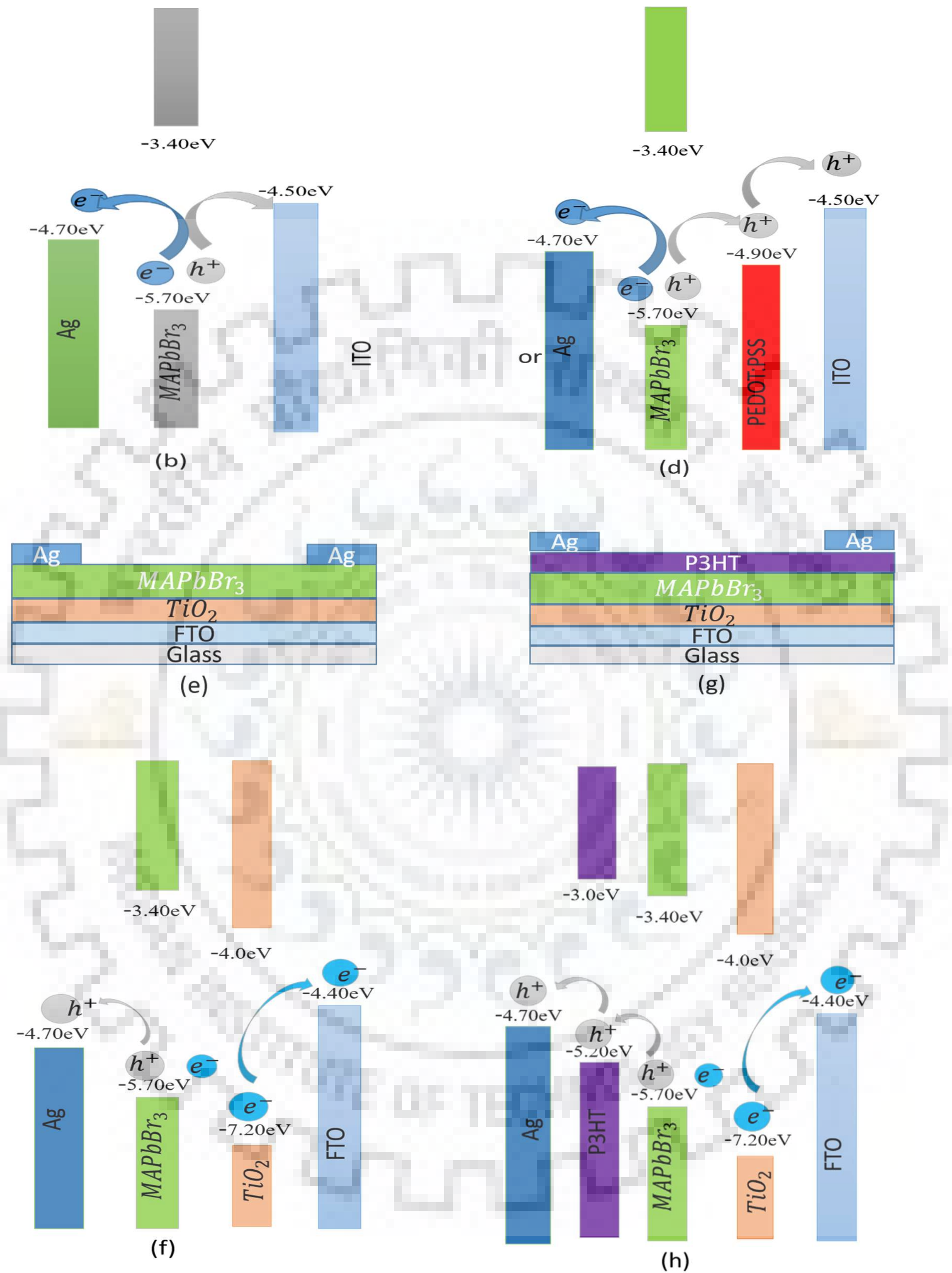

Fig-4.1 Schematic geometry of different combination and their energy band diagram with electron hole migration under reverse bias condition

3.Methodology

We have designed the photodiode in four different ways having slight change in in deposition technique for each one

(a) $ITO/MAPbBr_3/Ag$

Indium-doped tin oxide were etched with 2 M HCl and zinc powder. After this ITO substrate is cleaned by DI water with soap solution and it is sonicated for 15 in acetone and after this it is sonicated in iso-propyl alcohol to clean the substrate properly.

A 1.2 M solution of the perovskite precursors PbBr2 and MABr (1:1 ratio) was prepared in a solvent mixture of dimthylformaldihide (DMF) and dimethylsulfoxide (DMSO) in a 7:3 ratio. The precursor solution was deposited in a 3-step spin-coating program. The first step

of the program was at 500 rpm for 5s, the second step was at 1000 rpm for 40 s and the third step was at 5000 rpm for 50 s. At the beginning of the last step chlorobenzene was dripped on the substrate. Afterwards the films were annealed at 100 °C for 10 min.

After perovskite film deposition silver (Ag) electrode were deposited on the film by thermal vapour deposition technique.

(b) $ITO/PEDOT{:}PSS/MAPbBr_3/Ag$

Indium-doped tin oxide were etched with 2 M HCl and zinc powder. After this ITO substrate is cleaned by DI water with soap solution and it is sonicated for 15 in acetone and after this it is sonicated in iso-propyl alcohol to clean the substrate properly.

In this design PEDOT:PSS is spin coted on the cleaned ITO substrate first for 3000 rpm and 30 sec after this PEDOT:PSS coated film is annealed for 20 minute at 120℃. After this perovskite film is spin coated using A 1.2 M solution of the perovskite precursors PbBr2 and MABr (1:1 ratio) which was prepared in a solvent mixture of dimthylformaldihide (DMF) and dimethylsulfoxide (DMSO) in a 7:3 ratio. The precursor solution was deposited in a 3-step spin-coating program. The first step of the program was at 500 rpm for 5s, the second step was at 1000 rpm for 40 s and the third

Step was at 5000 rpm for 50 second. At the beginning of the last step chlorobenzene was dripped on substrate. Afterward the perovskite films were annealed at 100 °C for 10 min

for proper crystallization of perovskite thin film. After perovskite film deposition silver (Ag) electrode were deposited on the film by thermal vapour deposition technique.

(c) $FTO/TiO_2/MAPbBr_3/Ag$

Fluorine-doped tin oxide (FTO, Pilkington, 7 Ω^{-1}) substrates was etched with 2 M HCl and zinc powder The TiO2 layer was deposited via a sol-gel approach where a solution containing 0.23 M titanium isopropoxide (Sigma Aldrich, 99.999 %) and 0.013 M HCl in isopropanol was spin-coated on FTO at 2000 rpm for 30 s and annealed at 150 °C for 10 min and for 45 min at 500 °C for the FTO in ambient air conditions.

A 1.2 M solution of the perovskite precursors PbBr2 and MABr (1:1 ratio) was prepared in a solvent mixture of dimthylformaldihide (DMF) and dimethylsulfoxide (DMSO) in a 7:3 ratio. The precursor solution was deposited in a 3-step spin-coating program. The first step of the program was at 500 rpm for 5s, the second step was at 1000 rpm for 40 s and the third step was at 5000 rpm for 50 s. At the beginning of the last step chlorobenzene was dripped on the substrate. Afterwards the films were annealed at 100 °C for 10 min.

After perovskite film deposition silver (Ag) electrode were deposited on the film by thermal vapour deposition technique.

(d)$FTO/TiO_2/MAPbBr_3/P3HT/Ag$

Fluorine-doped tin oxide (FTO, Pilkington, 7 Ω^{-1}) substrates was etched with 2 M HCl and zinc powder The TiO2 layer was deposited via a sol-gel approach where a solution containing 0.23 M titanium isopropoxide (Sigma Aldrich, 99.999 %) and 0.013 M HCl in isopropanol was spin-coated on FTO at 2000 rpm for 30 s and annealed at 150 °C for 10 min and for 45 min at 500 °C for the FTO in ambient air conditions.

A 1.2 M solution of the perovskite precursors PbBr2 and MABr (1:1 ratio) was prepared in a solvent mixture of dimthylformaldihide (DMF) and dimethylsulfoxide (DMSO) in a 7:3 ratio. The precursor solution was deposited in a 3-step spin-coating program. The first step of the program was at 500 rpm for 5s, the second step was at 1000 rpm for 40 s and the third step was at 5000 rpm for 50 s. At the beginning of the last step chlorobenzene was dripped on the substrate. Afterwards the films were annealed at 100 °C for 10 min.

After perovskite film deposition a layer of p-type polymer Poly(3-hexylthiophene-2,5-diyl) (P3HT) is deposited on the perovskite film by spin coating at 1000 rpm for 30 sec. After deposition of all film silver (Ag) electrode were deposited on the film by thermal vapour deposition technique.

Fig-4.2 (1) Optical image of successive film deposited on substrates ITO and FTO (2) Optical image of perovskite photodiode for different geometry as mentioned above (a), (b), (c), (d),

4.Surface Morphology Characterization

To know the surface crystallization of the thin hybrid perovskite film on different substrate, it is used to follow some surface morphology characterization technique as Scanning Electron Microscope (SEM) and Atomic Force Microscope (AFM). These technique provides the information about the featured sized of crystalized crystals and morphological compactness of the deposited thin film, presence of pin hole in thin film

4.1 FE-SEM Characterization

We have used the scanning electron microscope technique to check film surface morphology and crystal shape and size of deposited perovskite thin fil on different substrate as shown below

(a) $ITO/MAPbBr_3$

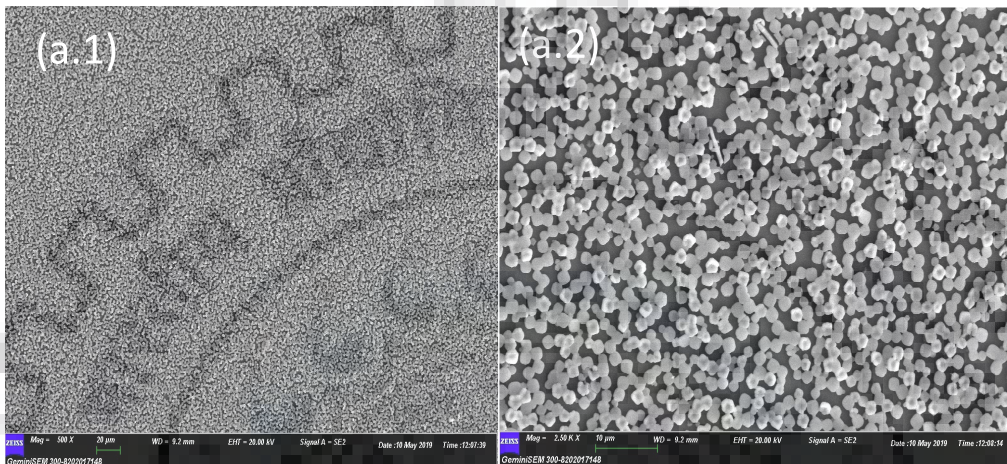

Fig-4.3 (a.1) for 20μm scale and (a.2) for 10μm scale, FE-SEM images of surface morphology for $ITO/MAPbBr_3$

(b) $ITO/PEDOT{:}PSS/MAPbBr_3$

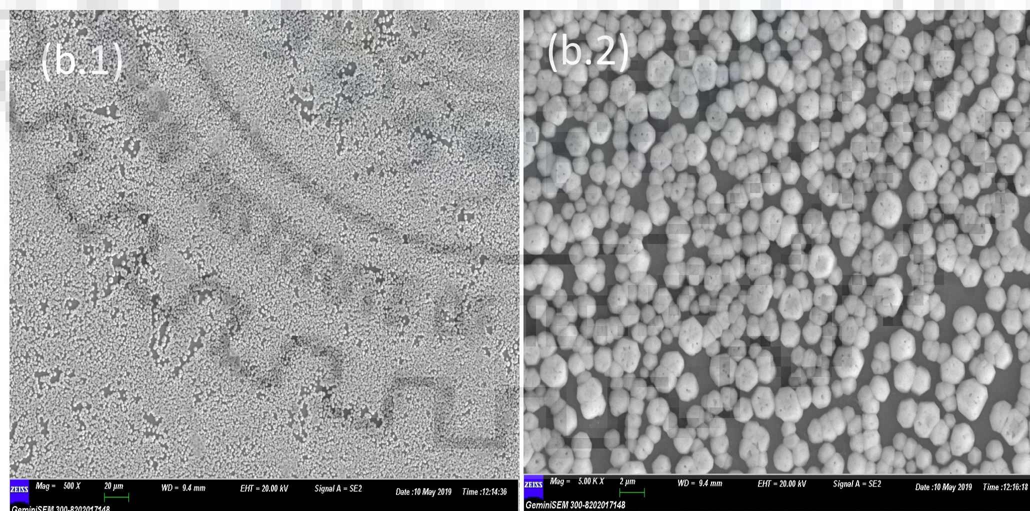

Fig-4.4 (b.1) for 20 μm scale and (b.2) for 10 μm scale FE-SEM images of surface morphology for $ITO/PEDOT{:}PSS/MAPbBr_3$

(c) $FTO/TiO_2/MAPbBr_3$

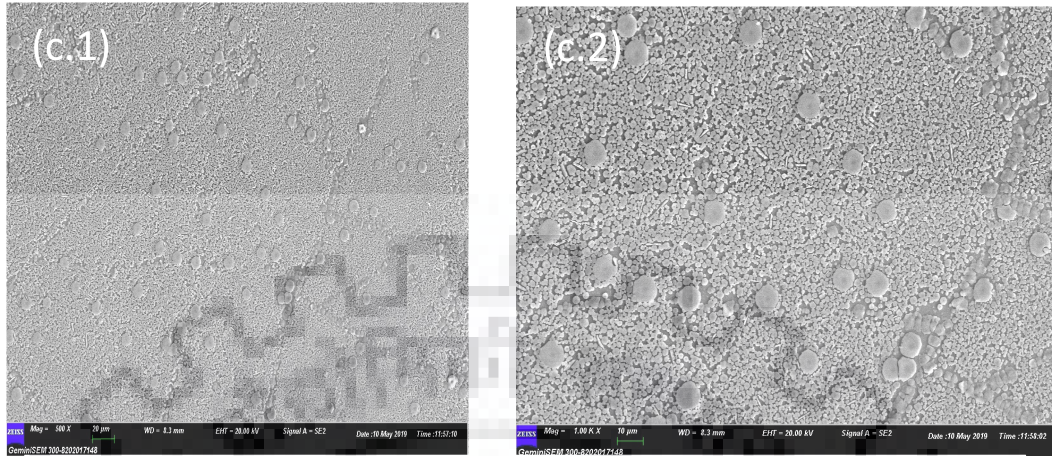

Fig-4.5 (c.1) for 20µm scale and (c.2) for 10µm scale FE-SEM images of surface morphology for $FTO/TiO_2/MAPbBr_3$

Discussion of FE-SEM characterization- In the case of ITO and PEDOT:PSS coated substrate hybrid perovskite $MAPbBr_3$ thin film is approximately 80% densely packed having average feature sized of single crystal 2µm but in case of TiO_2 coated FTO substrate perovskite film is approximately 80-85% densely packed but in this case some large crystal of 10µm size are crystalized and average feature sized of higher density small sized crystal is 2µm.

4.2 AFM Characterization

Surface morphology is studied for the composition perovskite photodiode also by Atomic Force Microscope (AFM) technique and the corresponding result are mentioned below-

(a) $ITO/MAPbBr_3$

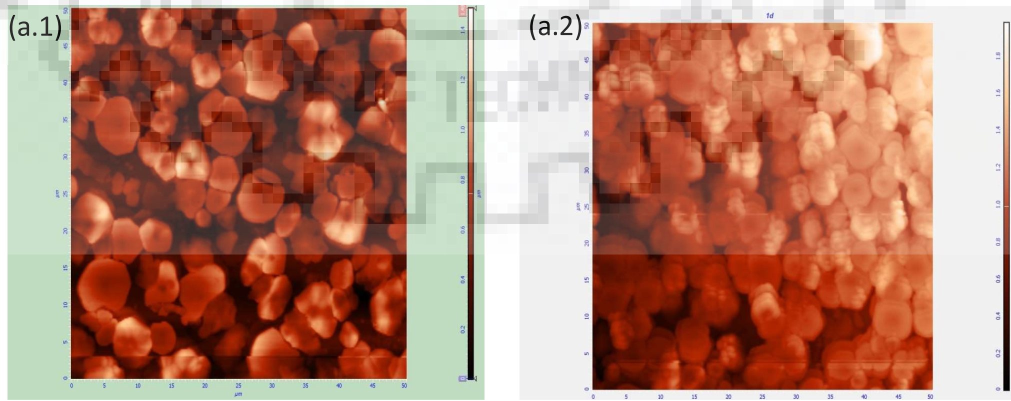

Fig-4.6 For 50µm (a.1) and (a.2) AFM images of surface morphology for $ITO/MAPbBr_3$

(b) $ITO/PEDOT:PSS/MAPbBr_3$

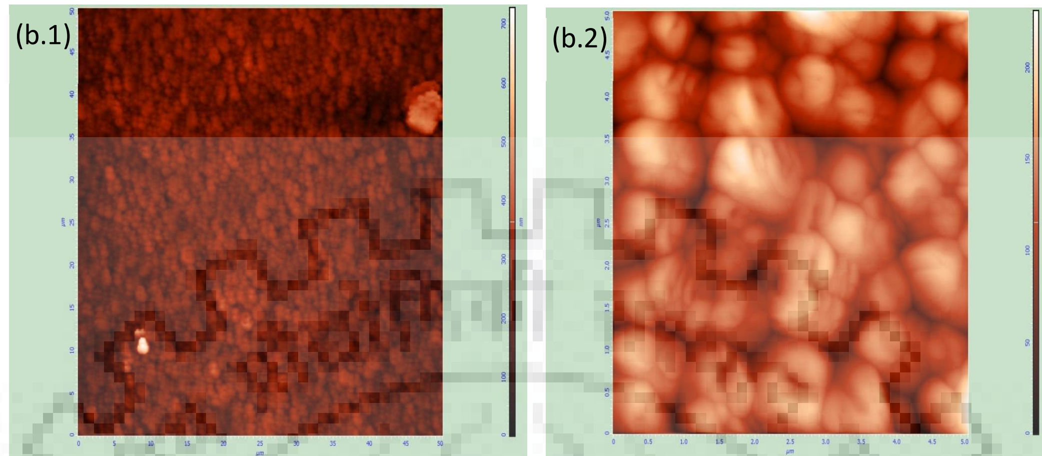

Fig-4.7 (b.1) for 50µm scale and (b.2) for 20µm scale, AFM images of surface morphology for $ITO/PEDOT:PSS/MAPbBr_3$

(c) $FTO/TiO_2/MAPbBr_3$

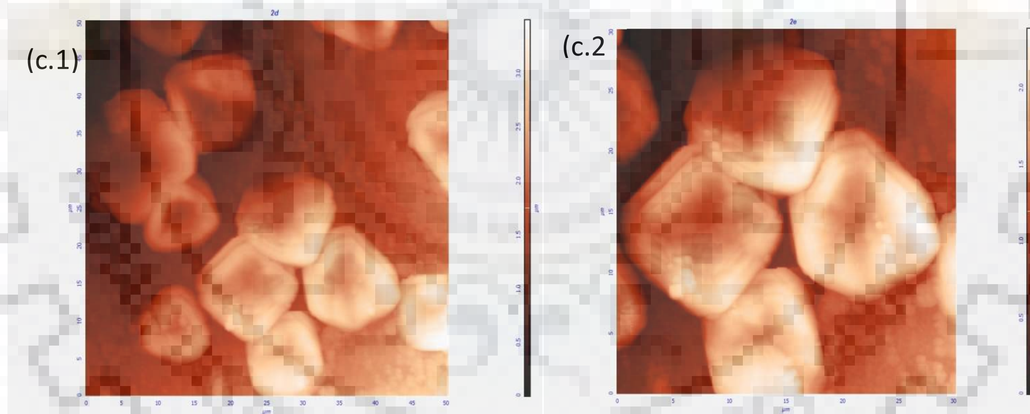

Fig-4.8 (c.1) for 50µm scale and (c.2) 20µm scale, AFM images of surface morphology for $FTO/TiO_2/MAPbBr_3$

Discussion of AFM characterization - In the case of ITO and PEDOT:PSS coated substrate hybrid perovskite $MAPbBr_3$ thin film is approximately 80% densely packed having average feature sized of single crystal 2µm but in case of TiO_2 coated FTO substrate perovskite film is approximately 80-85% densely packed but in this case some large crystal of 10µm size are crystalized and average feature sized of higher density small sized crystal is 2µm.

4.3 UV-Visible Absorption

We have recorded the absorbance of $MAPbBr_3$ film on different substrate and calculated the energy band gap of perovskite film using **Tauc plot** method

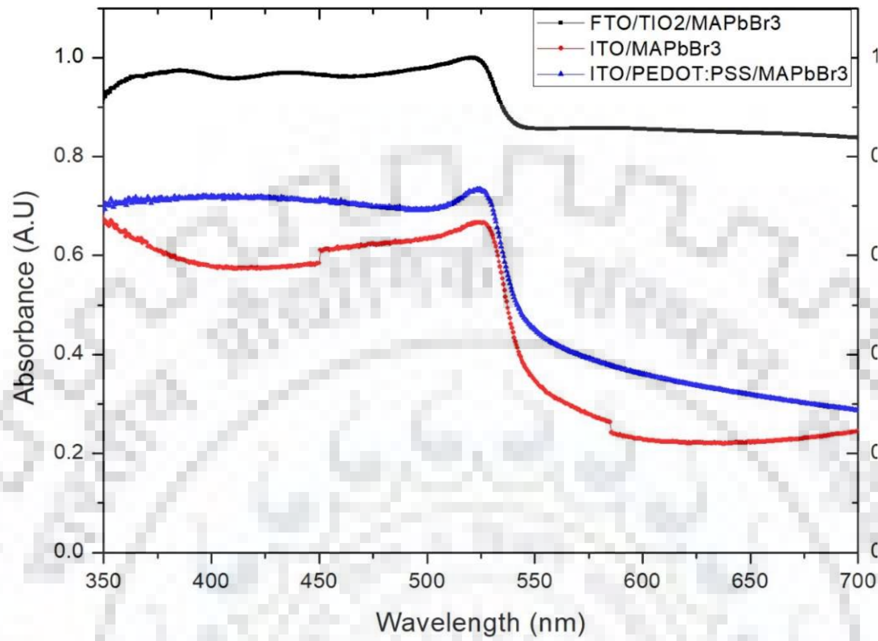

Fig-4.9 Absorbance spectrum of $MAPbBr_3$ film on different substrate as mentioned in graph

(a) $ITO/MAPbBr_3$

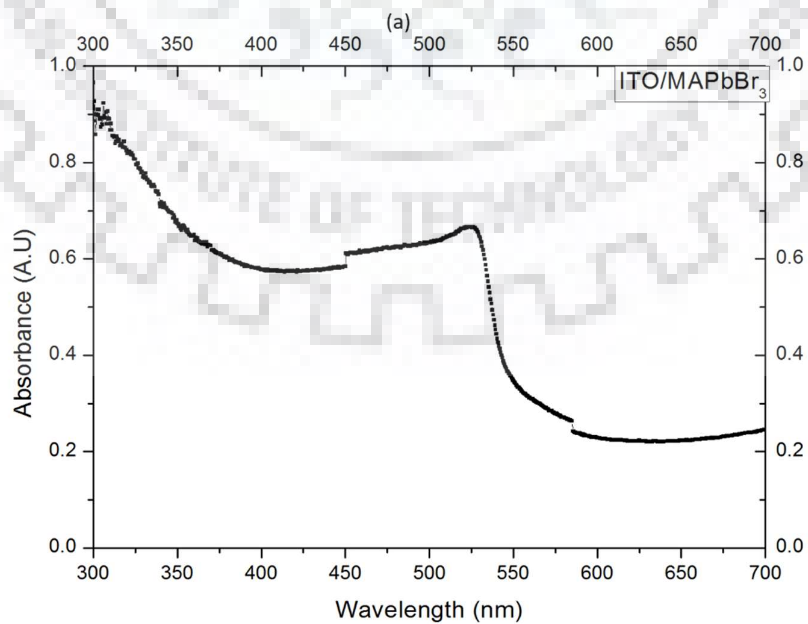

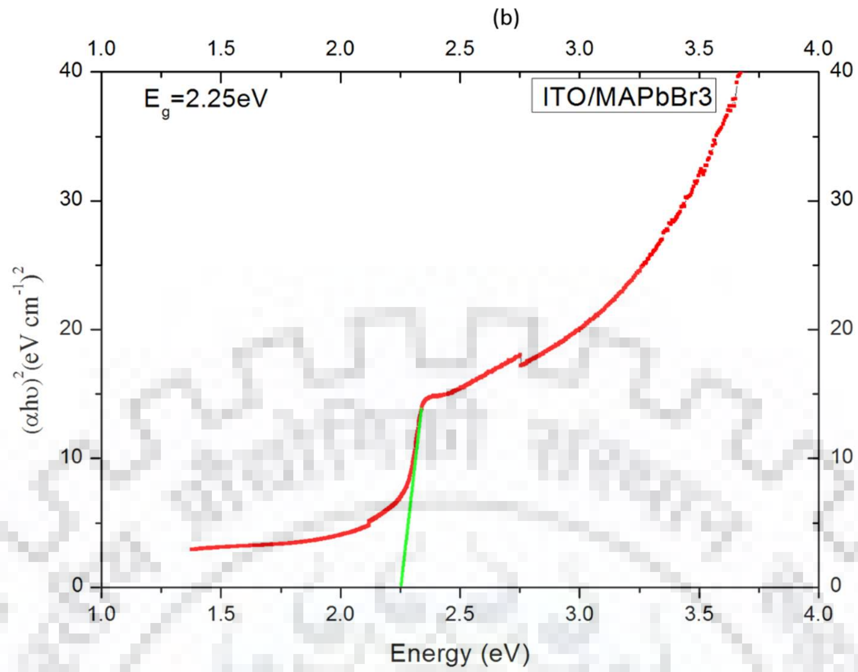

Fig-4.10 (a) Absorption spectrum of $MAPbBr_3$ film on ITO substrate and (b) Corresponding Tauc plot

(b) $ITO/PEDOT:PSS/MAPbBr_3$

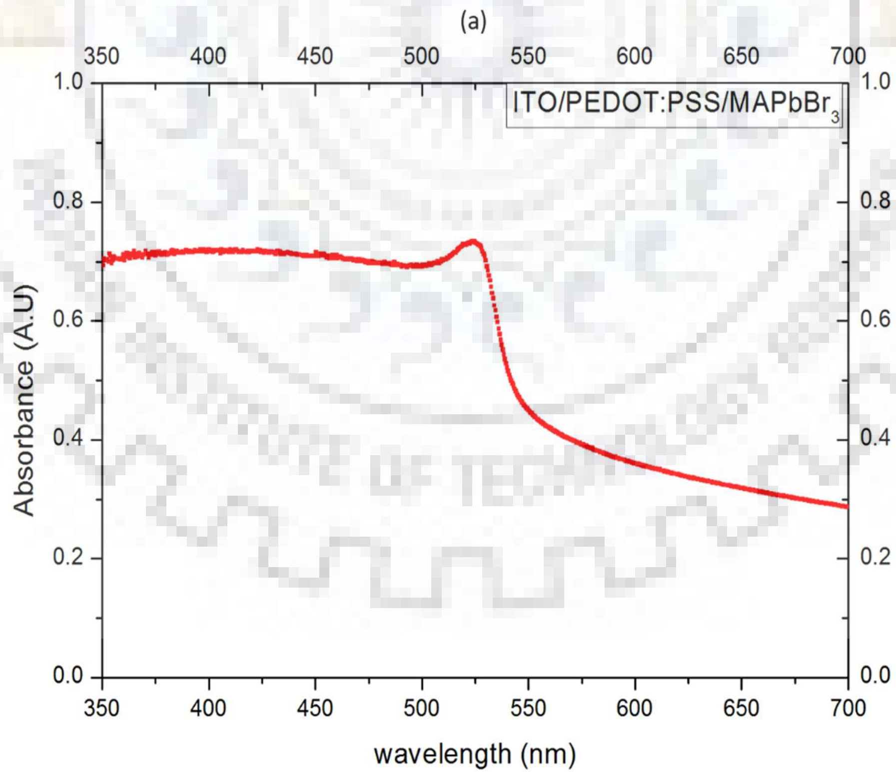

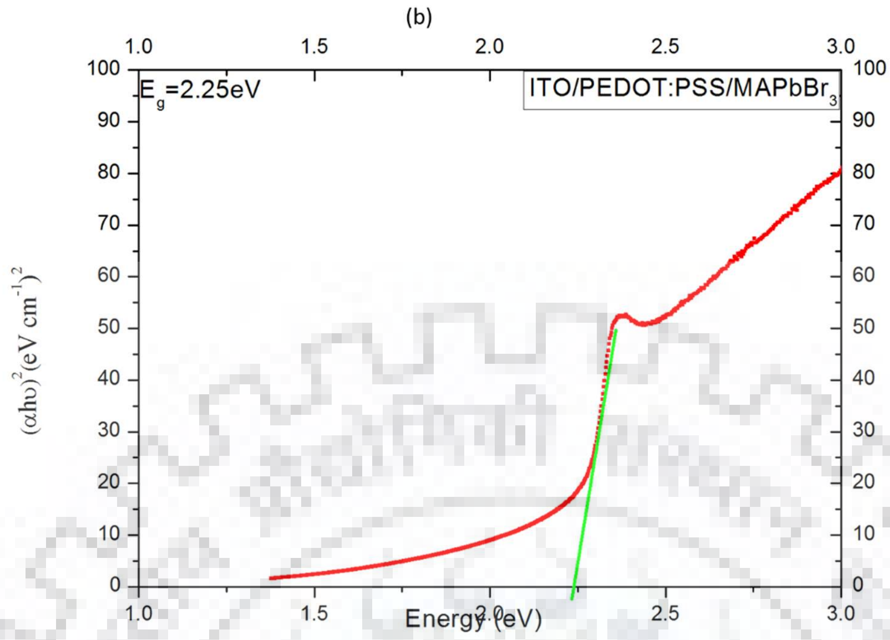

Fig-4.11 (a) Absorption spectrum of $MAPbBr_3$ film on PEDOT:PSS coated substrate and (b) Corresponding Tauc Plot

(c) $FTO/TiO_2/MAPbBr_3$

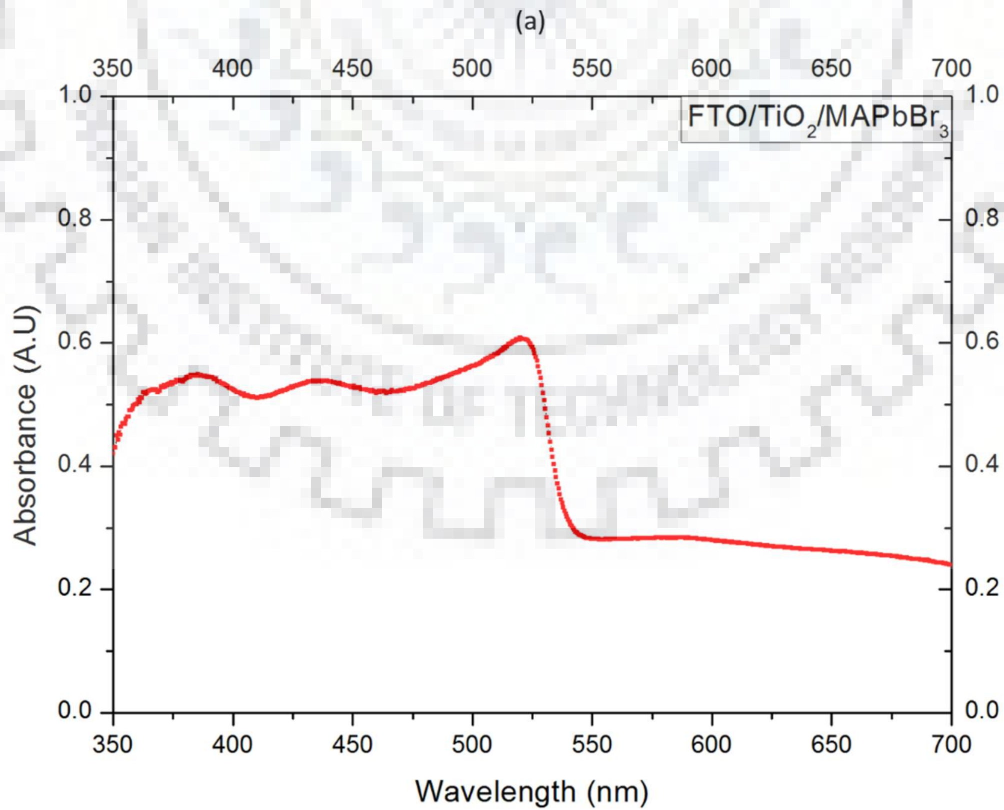

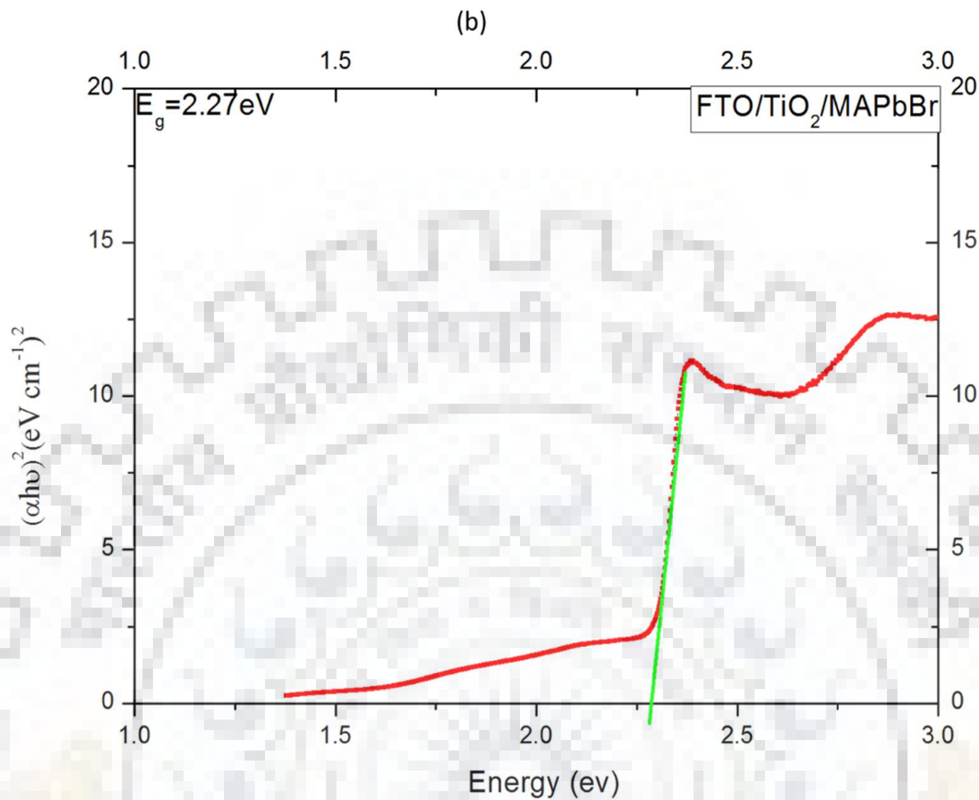

Fig-4.12 (a) Absorption spectrum of $MAPbBr_3$ film on TiO_2 coated FTO substrate and (b) Corresponding Tauc plot.

Discussion-It is verified by tauc plot of hybrid perovskite $MAPbBr_3$ thin film is 2.25eV to 2.5 eV as reported previously for different substrate as shown in above mentioned graph and fig-3.13 represents that for different substrate $MAPbBr_3$ film shows the different absorptivity same light under UV-Visible spectrum. .

4.Electrical characterization

We have fabricated different hybrid perovskite $MAPbBr_3$ thin film based photodetector using different substrate. Such devices are biased in forward under voltage range -5V to +5V under forward bias forward device current flows and reverse bias condition for 0V to -5V under illumination of green to produce photocurrent across it.

4.1 I-V Under forward bias

We have fabricated different hybrid perovskite $MAPbBr_3$ thin film based photodetector using different substrate. Such devices are biased in forward under voltage range -5V to +5V under forward bias forward device current flows in devices as shown

(a) $ITO/PEDOT:PSS/MAPbBr_3$/Ag

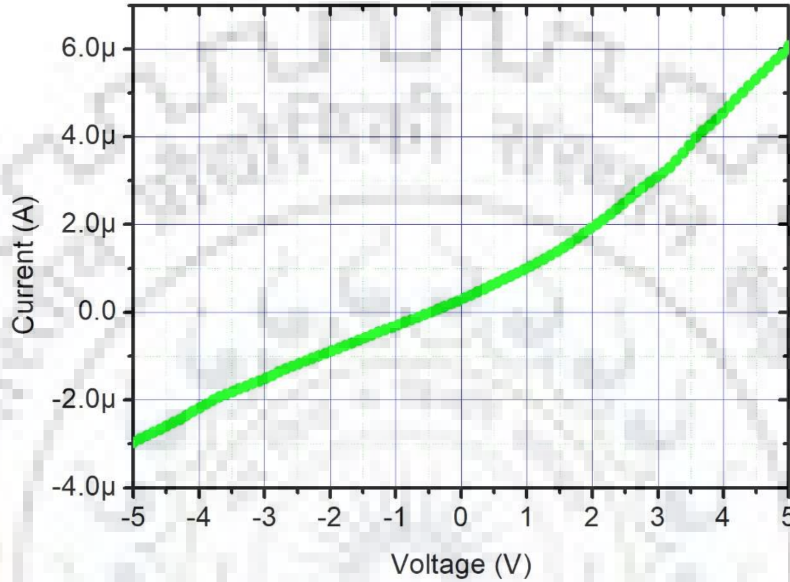

(b) $FTO/TiO_2/MAPbBr_3$/Ag

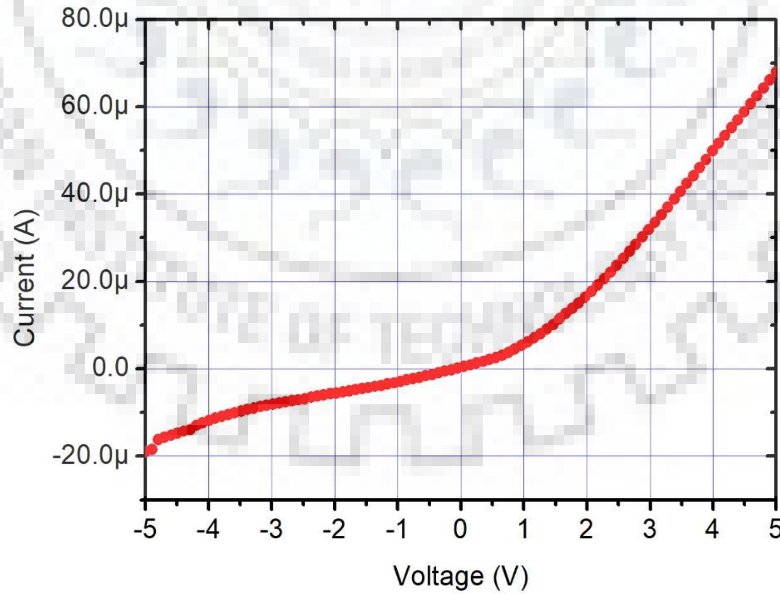

Fig-4.13 (a) and (b) I-V characteristics of perovskite devices under the range -5V to 5V.

4.2 Photocurrent Generation

Such devices can be used as photodetector under reverse bias condition as presented the graph given below because it is predicted from the graph 3.12 (a) and (b) having I-V characteristics as like normal P-n junction diode.

$(a)\ ITO/PEDOT{:}PSS/MAPbBr_3$/Ag

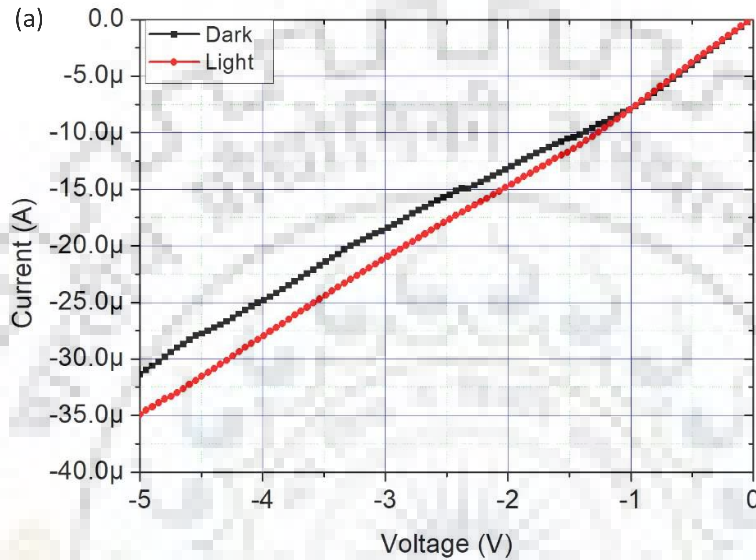

(b) $FTO/TiO_2/MAPbBr_3$/Ag

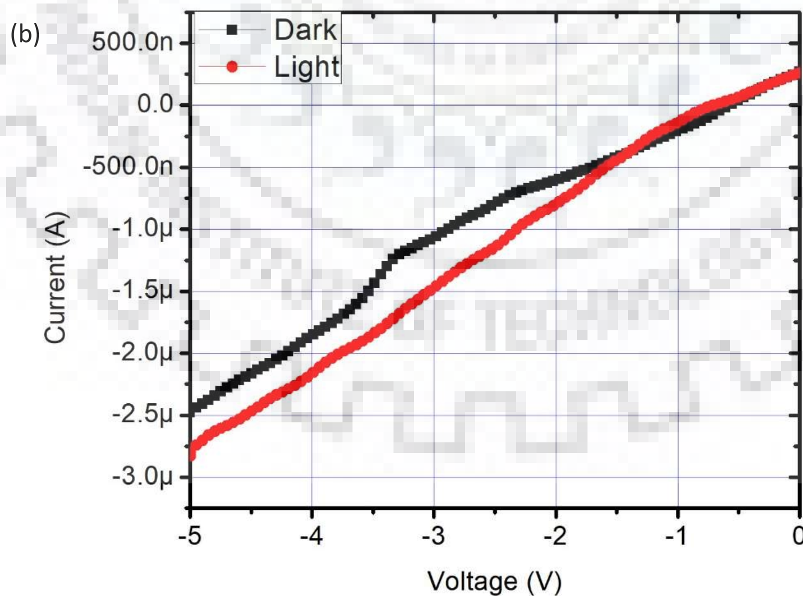

Fig-4.14 (a) and (b) Photocurrent generation in perovskite devices under the light illumination in reverse bias condition for 0V to -5V biasing range.

5. Degradation of $MAPbBr_3$ Perovskite film under Direct Illumination of Light

To see the effect of light directly on perovskite thin film we made an incidence of green laser light directly perovskite film for different light intensity

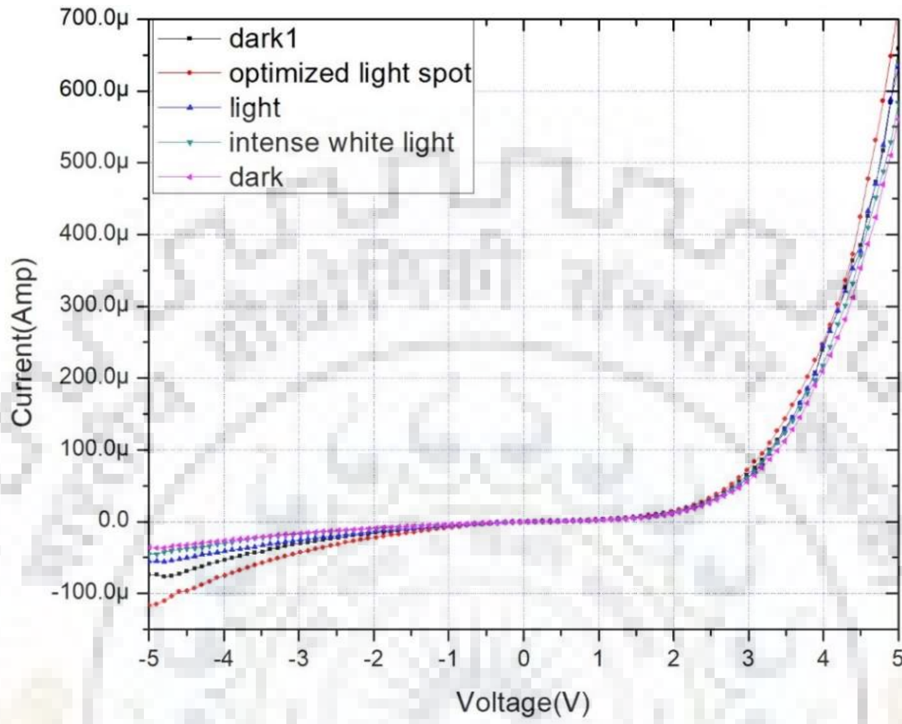

Fig-4.15 Direct effect of light on hybrid perovskite film

It is verified when light directly make an incidence on hybrid perovskite film, Perovskite film degrades because of thermal degradation caused by direct light on it. It is concluded from the I-V characteristics of the perovskite devices under forward bias from 0V to 5V or -5V to +5V is as simple P-N junction diode. It has lateral photoconductive geometry for the top two electrode with common back electrode. Figure 4.13 (a) is the I-V characteristics for simple p-i-n device structure and figure 4.13 (b) represents I-V characteristics for simple n-i-p device structure so the polarity of charge flow is different for both device structures. Such devices are used as photodetector under reverse bias condition under the illumination of green laser light. Green laser light is used for illumination of device because the energy band gap of hybrid perovskite $MAPbBr_3$ is 2.25 eV or lies in the range of 2.2 eV to 2.5 eV and the energy of green light photon is equal or more than this energy band gap range of hybrid perovskite film, such photons are absorbed in the energy band gap region to generate the photo-current across the devices which is verified by the figure 4.14 (a) and (b).

CHAPTER-5

CONCLUSION & FUTURE SCOPE

1.CONCLUSION

It is concluded by the result of strain induced in PDMS flexible grating having grating pitch 1.4µm and 0.7µm and grating depth 160nm and 50nm respectively, these grating works in reliable mode under the range of applied pressure 0 to 0.3945MPa and 0 to 0.337692MPa with the Sensitivity =0.0263MPa^{-1}. Such gratings will work as deflection diaphragm for compact purposed sensor design. Figure 5.15 (a) is the I-V characteristics for simple p-i-n device structure and figure 5.15 (b) represents I-V characteristics for simple n-i-p device structure so the polarity of charge flow is different for both device structures. Such devices are used as photodetector under reverse bias condition under the illumination of green laser light. Green laser light is used for illumination of device because the energy band gap of hybrid perovskite $MAPbBr_3$ is 2.25 eV or lies in the range of 2.2 eV to 2.5 eV and the energy of green light photon is equal or more than this energy band gap range of hybrid perovskite film, such photons are absorbed in the energy band gap region to generate the photocurrent across the devices which is verified by the graph 5.16 (a) and (b). It is predicted that the devices having different substrate have different photocurrent induced across the device due to the crystallization of different feature sized crystal with different substrate and for PEDOT:PSS coated substrate more photocurrent is generated because thin PEDOT:PSS film remove passivation defects for crystallization of more compact perovskite film growth.

PDMS grating as transducer and hybrid perovskite $MAPbBr_3$ based photodiode will be integrated according to the purposed design of **Low Cost Optical Pressure Sensor Having Flexible Grating.**

2 Future Scope

Such type of flexible Grating made by polymers as PDMS are very useful in various field of science and research such as sensor technology

(a) **Microscopic imaging**
Microscopic imaging using its pixels formation to get enhanced magnification of images of microscopic objects.

(b) **TE-TM Polarization detection-**
When polarized light falls on the PDMS Grating it shows different type of result as given below

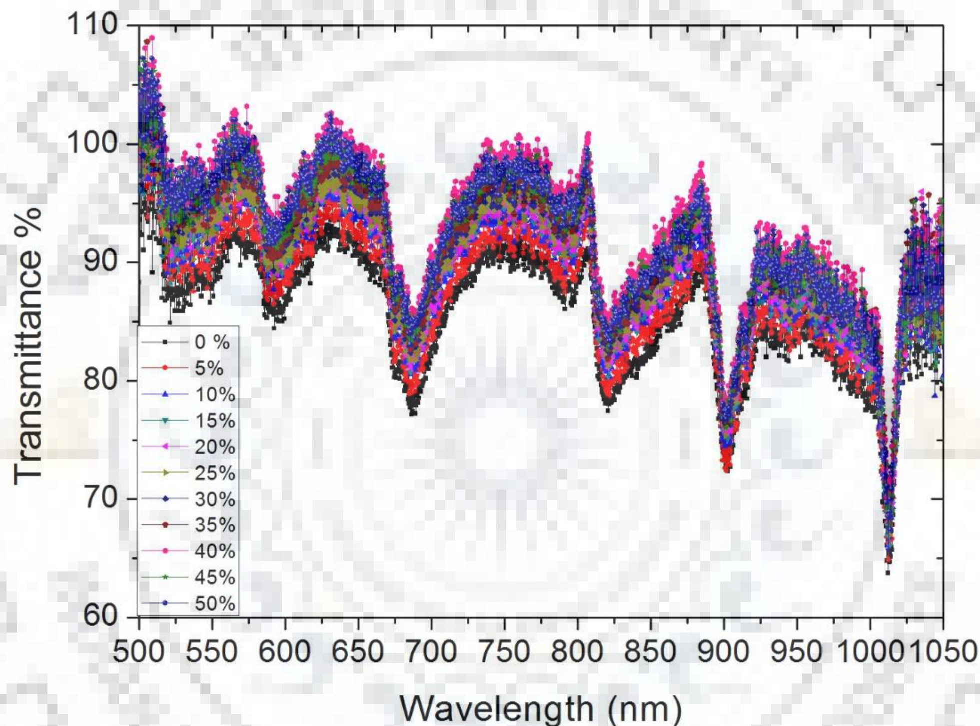

When TM polarized light, considering TE polarization as reference, falls on the PDMS Grating having grating pitch 0.7μm and strain is induced from 0% to 50%, Different order dips are found at various wavelength. As the induced strain PDMS Grating is increased these observed dips are shifting upward.
By the literature survey for such behaviour it is found the such type of flexible Grating can be used as

(1) Selective wavelength filter
(2) In Guided Mode Resonance using like strip wave guide
(3) In Bio sensing.

Bibliography

[1] D. Estrin, R. Govindan, J. Heidemann, S. Kumar, "Next century challenges: Scalable coordination in sensor networks", *Proc. Int. Conf. Mobile Computing and Networking (MOBICOM),* pp. 263-270, 1999.

[2] G. Berruti, M. Consales, M. Giordano, L. Sansone, P. Petagna, S. Buontempo, G. Breglio and A. Cusano, Radiation hard humidity sensors for high energy physics applications using polyimide-coated fiber Bragg gratings sensors, Sensors and Actuators B 177 ,94–102 (2013).

[3] T. Vo-Dinh and B. Cullum, Biosensors and biochips: advances in biological and medical diagnostics, Fresenius' Journal of Analytical Chemistry 366 ,540–551(2000).

[4] R. Polsky, J.C. Harper, D.R. Wheeler, S.M. Dirk, D.C. Arango and S.M. Brozik, Electrically addressable diazonium-functionalized antibodies for multianalyte electrochemical sensor applications, Biosensors and Bioelectronics 23,757–764 (2008).

[5] Someya, T. *et al. Conformable, flexible, large-area networks of pressure and thermal sensors with organic transistor active matrixes*. *Proc. Natl Acad.* Sci. **102**, 12321–12325 (2005).

[6] Someya, T. *et al. A large-area, flexible pressure sensor matrix with organic field-effect transistors for artificial skin applications*. *Proc. Natl Acad*. Sci. **101**, 9966–9970 (2004).

[7] Xiaoshuang Duan, Jiangjiang Luo, Yanbo Yao, and Tao Liu . A Route toward Ultrasensitive Layered Carbon Based Piezoresistive Sensors through Hierarchical Contact Design. *ACS Applied Materials & Interfaces***,** *9* (49) , 43133-43142 (2017).

[8] Hyejin Hwang, Song-Ee Choi, Sang Woo Han, Insang You, Eun Sook Jeong, Sinae Kim, Hakyeong Yang, Sangyeop Lee, Jaebum Choo, Jin Woong Kim, Unyong Jeong. Cut-and-Paste Transferrable Pressure Sensing Cartridge Films. *Chemistry of Materials***,** *30* (18) , 6410-6419 (2018).

[9] Sagar M. Doshi, Erik T. Thostenson. Thin and Flexible Carbon Nanotube-Based Pressure Sensors with Ultrawide Sensing Range. *ACS Sensors***,** *3* (7) , 1276-1282, (2018).

[10] Dennis Alveringh, Remco J. Wiegerink, Joost C. Lötters, "Integrated Pressure Sensing Using Capacitive Coriolis Mass Flow Sensors", *Microelectromechanical Systems Journal of*, vol. 26, no. 3, pp. 653-661, (2017).

[11] Xiuchun Hao, Sinya Tanaka, Atsuhiko Masuda, Jun Nakamura, Koichi Sudoh, Kazusuke Maenaka, Hidekuni Takao, Kohei Higuchi, Application of Silicon on Nothing Structure for Developing a Novel Capacitive Absolute Pressure Sensor, *Sensors Journal IEEE*, vol. 14, no. 3, pp. 808-815, (2014).

[12] Ananiah Durai Sundararajan, S. M. Rezaul Hasan, Elliptic Diaphragm Capacitive Pressure Sensor and Signal Conditioning Circuit Fabricated in SiGe CMOS Integrated MEMS, *Sensors Journal IEEE*, vol. 15, no. 3, pp. 1825-1837, (2015).

[13] Li, J., Wang, C., Ma, J. & Liu, M. *Micromachined ultrasonic transducers based on lead zirconate titanate (PZT) films*. *Microsyst. Technol.* **19**, 211–218 (2013).

[14] Maeda, R., Tsaur, J. J., Lee, S. H. & Ichiki, M. *Piezoelectric microactuator devices*. *J. Electroceram.* **12**, 89–100 (2004).

[15] Zarnik, M. S., Belavič, D., Maček, S. & Holc, J. *Feasibility study of a thick-film PZT resonant pressure sensor made on a prefired 3D LTCC structure*. *Int. J. Appl. Ceram. Technol.* **6**, 9–17 (2009).

[16] Damjanovic, D. *Ferroelectric, dielectric and piezoelectric properties of ferroelectric thin films and ceramics*. *Rep. Prog. Phys.* **61**, 1267–1324 (1998).

[17] Hussain, M., Choa, Y-H. & Niihara, K. *Conductive rubber materials for pressure sensors*. *J. Mater. Sci. Lett.* **20**, 525–527 (2001).

[18] Joint Assessment of Commodity Chemicals, September (Report No. 26) ISSN 0773-6339-26,(1994).

[19] Mark, J. E.; Allcock, H. R.; West, R. "Inorganic Polymers" Prentice Hall, Englewood, NJ: ISBN 0-13-465881-7,(1992).

[20] Lotters, J. C.; Olthuis, W.; Veltink, P. H.; Bergveld, P. The mechanical properties of the rubber elastic polymer polydimethylsiloxane for sensor applications. J Micromech Microeng. 7 (3): 145–147 (1997).

[21] L.H. Sperling, Introduction to Physical Polymer Science, Wiley-Interscience, New Jersey, 2006.

[22] Wang, Zhixin, "Polydimethylsiloxane Mechanical Properties Measured by Macroscopic Compression and Nanoindentation Techniques" 3402 (2011).

[23] koschwanez jh, Carlson RH, Meldurm DR thin film PDMS using spin times or Tert Butyl Alcohol as solvent 1371/.0004572 (2009).

[24] Nanoindentation methods and critical aspects of interpreting results to assess PDMS mechanical properties. V C 2014 Wiley Periodicals, Inc. J. Appl. Polym. Sci, 131, 41384, (2014).

[25] Lee, H-K., Chang, S-I. & Yoon, E. *A flexible polymer tactile sensor: Fabrication and modular expandability for large area deployment*. *J. Microelectromech. Syst.* **15**, 1681–1686 (2006).

[26] Metzger, C. *et al. Flexible-foam-based capacitive sensor arrays for object detection at low cost*. *Appl. Phys. Lett.* **92**, 013506 (2008).

[27] Shirinov, A. V. & Schomburg, W. K. *Pressure sensor from a PVDF film*. *Sens. Actuat. A* **142**, 48–55 (2008).

[28]Reese, C., Chung, W-J., Ling, M-M., Roberts, M. E. & Bao, Z. *High-performance microscale single-crystal transistors by lithography on an elastomer dielectric*. *Appl. Phys. Lett.* **89**, 202108 (2006).

[29] Chan, Y., Mi, Y., Trau, D., Huang, P. & Chen, E. *Micromolding of PDMS scaffolds and microwells for tissue culture and cell patterning: A new method of microfabrication by the self-assembled micropatterns of diblock copolymer micelles*. *Polymer* **47**, 5124–5130 (2006).

[30] G. R. Harrison and E. G. Loewen, "Ruled gratings and wavelength tables," Appl. Opt. 15, 1744-1747 (1976).

[31] G. R. Harrison and G. W. Stroke, "Interferometric control of grating ruling with continuous carriage advance," J. Opt. Soc. Am. 45, 112-121 (1955).

[32] N. Abramson, "Principle of least wave change," J. Opt. Soc. Am. A6, 627-629 (1989).

[33] Brunner, K. et al. Sharp-line photoluminescence and two-photon absorption of zero-dimensional biexcitons in a GaAs/AlGaAs structure. *Phys. Rev. Lett.* **73**, 1138–1141 (1994).

[34] Alferov, Z. I. Nobel Lecture: The double heterostructure concept and its applications in physics, electronics, and technology. *Rev. Mod. Phys*. **73**, 767–782 (2001).

[35] N. Teranishi, A. Kohono, Y. Ishihara, E. Oda, K. Arai, "No image lag photodiode structure in the interline CCD image sensor", *IEDM Tech. Dig.*, pp. 324-327, 1982.

[36] C. Mead, Analog VLSI and Neural Systems, MA, Reading:Addison Wesley, 1989.

[37] Dou, L. *et al.* Solution-processed hybrid perovskite photodetectors with high detectivity. *Nat. Commun.* 5:5404, (2014).

[38] Saidaminov, M. I. *et al*. Planar-integrated single-crystalline perovskite photodetectors. *Nat. Commun.* 6:8724 doi: 10.1038/ncomms9724 (2015).

[39] Tan, Z.-K. *et al.* Bright light-emitting diodes based on organometal halide perovskite. *Nat. Nanotechnol.* **9**, 687–692 (2014).

[40] Li, G. *et al.* Efficient light-emitting diodes based on nano-crystalline perovskite in a dielectric polymer matrix. *Nano Lett.* **15**, 2640–2644 (2015).

[41] Yang, W. S. *et al.* High-performance photovoltaic perovskite layers fabricated through intermolecular exchange. *Science* **348**, 1234–1237 (2015).

[42] Stranks, S. D. *et al.* Electron-hole diffusion lengths exceeding 1 micrometer in an organometal trihalide perovskite absorber. *Science* **342**, 341–344 (2013).

[43] Lingliang Li, Yehao Deng, Chunxiong Bao, Yanjun Fang, Hotong Wei, Shi Tang, Fujun Zhang, Jinsong Haung "Self-Filtered Narrowband Perovskite Photodetectors with Ultrafast and Tuned Spectral Response" Advanced optical materials ,201700672 (2017),

[44] Z. Cheng, J. Lin, Layered organic–inorganic hybrid perovskites: structure, optical properties, film preparation, patterning and templating engineering, CrystEngComm, 2646-2662,12 (2010).

[45] N. Ramadass, ABO3-type oxides—Their structure and properties—A bird's eye view, Materials Science and Engineering, 36 231-239 (1978).

[46] Stokes, Debbie J.Principles and Practice of Variable Pressure Environmental Scanning Electron Microscopy (VP-ESEM). Chichester: John Wiley & Sons. ISBN 978-0470758748, (2008).

[47] Baghaei Rad, Leili; Downes, Ian; Ye, Jun; Adler, David; Pease, R. Fabian W. "Economic approximate models for backscattered electrons, Journal of Vacuum Science and Technology. **25** (6): 2425, (2007).

[48] Binnig, G.; Quate, C. F.; Gerber, C. (1986). "Atomic Force Microscope". *Physical Review Letters*. **56** (9): 930–933, (1986).

[49] Interdorfer, P; Dufrêne, Yf , Detection and localization of single molecular recognition events using atomic force microscopy, Nature Methods. **3** (5): 347–55, (May 2006).

[50] S. Middleman and A.K. Hochberg. "Process Engineering Analysis in Semiconductor Device Fabrication". McGraw-Hill, p. 313 (1993).